NO–β-catenin crosstalk modulates primitive streak formation prior to embryonic stem cell osteogenic differentiation

Huawen Ding[1,*], Kevin C. Keller[2], Ivann K. C. Martinez[2], Rose M. Geransar[3], Kai O. zur Nieden[2], Sandra G. Nishikawa[3], Derrick E. Rancourt[3] and Nicole I. zur Nieden[1,2,3,*,‡]

[1]Fraunhofer Institute for Cell Therapy and Immunology, Applied Stem Cell Technologies Unit, 04103 Leipzig, Germany
[2]Department of Cell Biology and Neuroscience, and Stem Cell Center, University of California Riverside, Riverside, CA, 92521, USA
[3]Institute of Maternal and Child Health, University of Calgary, Calgary, AB, Canada, T2N 4N1

*These authors contributed equally to this work
‡Author for correspondence (nicole.zurnieden@ucr.edu)

Accepted 21 June 2012
Journal of Cell Science 125, 5564–5577

doi: 10.1242/jcs.081703

Summary

Nitric oxide (NO) has been shown to play a crucial role in bone formation *in vivo*. We sought to determine the temporal effect of NO on murine embryonic stem cells (ESCs) under culture conditions that promote osteogenesis. Expression profiles of NO pathway members and osteoblast-specific markers were analyzed using appropriate assays. We found that NO was supportive of osteogenesis specifically during an early phase of *in vitro* development (days 3–5). Furthermore, ESCs stably overexpressing the inducible NO synthase showed accelerated and enhanced osteogenesis *in vitro* and in bone explant cultures. To determine the role of NO in early lineage commitment, a stage in ESC differentiation equivalent to primitive streak formation *in vivo*, ESCs were transfected with a T-brachyury–GFP reporter. Expression levels of T-brachyury and one of its upstream regulators, β-catenin, the major effector in the canonical Wnt pathway, were responsive to NO levels in differentiating primitive streak-like cells. Our results indicate that NO may be involved in early differentiation through regulation of β-catenin and T-brachyury, controlling the specification of primitive-streak-like cells, which may continue through differentiation to later become osteoblasts.

Key words: Nitric oxide, Embryonic stem cell, Brachyury, β-catenin, Osteoblast, Primitive streak

Introduction

Mouse and human embryonic stem cells (ESCs) are capable of differentiating into osteoblasts in the presence of ascorbic acid and β-glycerophosphate (Buttery et al., 2001; Phillips et al., 2001; Sottile et al., 2003); this differentiation can be enhanced using dexamethasone or 1α,25-OH_2 vitamin D_3 (VD_3) as osteogenic triggers (Buttery et al., 2001; zur Nieden et al., 2003). The osteogenic differentiation program can be divided into distinct temporal phases, in which osteoblasts either specify from a mesodermal population or an ectoderm-derived neural crest origin (Keller and zur Nieden, 2011), both of which are committed during embryogenesis as the primitive streak undergoes formation.

Now that ESC osteoblast differentiation has been demonstrated by a number of groups, research has shifted towards the identification of factors, which improve osteoblast output. This is of special importance since resulting cells can be used in cell-based regenerative therapies of degenerative bone diseases. Recently, we have used expression microarrays to identify pathways associated with osteoblast differentiation in order to improve the efficiency of directed differentiations (zur Nieden et al., 2007a). We have begun to map out a pattern of growth factor families, which when applied in specific order lead to a significant enhancement in osteoblast output, from ~60 to >90%.

Nitric oxide (NO) was one pathway that we identified during this previous study. NO is a special signaling molecule, being a highly reactive free radical with a short half-life. It can act within the cell where it is produced or penetrate cell membranes to affect adjacent cells. The effects of NO extend to smooth muscle relaxation, vasodilation, excitotoxicity, and the regulation of protein activity through S-nitrosylation. NO is known to play an important role in bone homeostasis; it is generated by many cell types present in the bone environment, most notably, the osteoblast (Evans and Ralston, 1996). In ESCs, NO donors are known to promote general differentiation (Mora-Castilla et al., 2010) and cardiomyogenesis in particular (Mujoo et al., 2008; Padmasekar et al., 2011).

NO is synthesized from L-arginine by three isozymes of nitric oxide synthase (NOS), including: neuronal NOS (nNOS), endothelial (constitutive) NOS (eNOS) and cytokine-inducible NOS (iNOS). Both iNOS and eNOS have been found to play roles in osteoblast differentiation. High concentrations of NO release resulting from pathological iNOS expression is thought to promote bone resorption and bone formation (Lin et al., 2003; Chae et al., 1997) by reducing osteoblast activity (Hukkanen et al., 1995). In contrast, during development eNOS is constitutively expressed by osteoblast-like cells. It has been shown that mice lacking eNOS have marked bone abnormalities due to impaired osteoblast differentiation resulting in poor maintenance of bone mass (Aguirre et al., 2001; Armour et al., 2001). RT-PCR of neonatal calvarial osteoblasts from $eNOS^{-/-}$ mice has shown downregulation of Cbfa-1 and osteocalcin (Afzal et al., 2004).

In this study, we have sought to determine whether appreciable differences in ESC osteoblast differentiation can result from NO augmentation at different phases during osteogenesis *in vitro*. We investigated the effect of supplementing NO/NOS agonists and/or antagonists throughout the course of ESC cultures. Since many of our previously identified pathways impinged upon nuclear β-catenin (CatnB) signaling, which plays an important role in ESC osteogenesis (zur Nieden et al., 2007; Davis and zur Nieden, 2008), we also looked to elucidate the effect of specific NOS isoforms in differentiation and to pinpoint a possible mechanism for the effect of NO on osteogenesis through the regulation of the Wnt/CatnB pathway.

Results

Temporal expression pattern of NO pathway members

A comprehensive microarray study performed using VD_3-induced osteoblast cultures previously suggested that NO played a role in early ESC osteogenesis (zur Nieden et al., 2007a). To confirm this role, in the current study we closely examined the gene expression pattern of molecules involved in NO synthesis and metabolism within the first 16 days after differentiation induction. Throughout these first 2 weeks of culture gene expression analysis showed temporal differences in the basal expression levels of both the eNOS and iNOS enzymes that synthesize NO (Fig. 1A). eNOS expression levels increased after day 8; increases in iNOS expression were also pronounced, with maximal expression of iNOS occurring between days 4 and 5. This specific regulation of iNOS mRNA occurred during the spontaneous differentiation induction of the cells in control medium, which is induced by removal of LIF. During the first five differentiation days, which is before the addition of VD3, progenitors of all three germ layers are specified (Chen et al., 1992) a subpopulation of which then responds to the osteogenic induction (zur Nieden et al., 2003).

In addition to NOS, we also inspected the mRNA levels of the dimethylarginine dimethylaminohydrolase enzyme, Ddah2. Ddah2 was identified as being involved in ESC osteogenic differentiation in our previous microarray screen (zur Nieden et al., 2007a) and has been described to play a role in NO synthesis through its function as a degrading enzyme of asymmetric dimethylarginine (ADMA), an endogenous arginine that inhibits the synthesis of NO (Ogawa et al., 1987; Ogawa et al., 1989; Leiper et al., 1999). Therefore, transcriptional regulation of Ddah2 may alter NO synthesis as previously

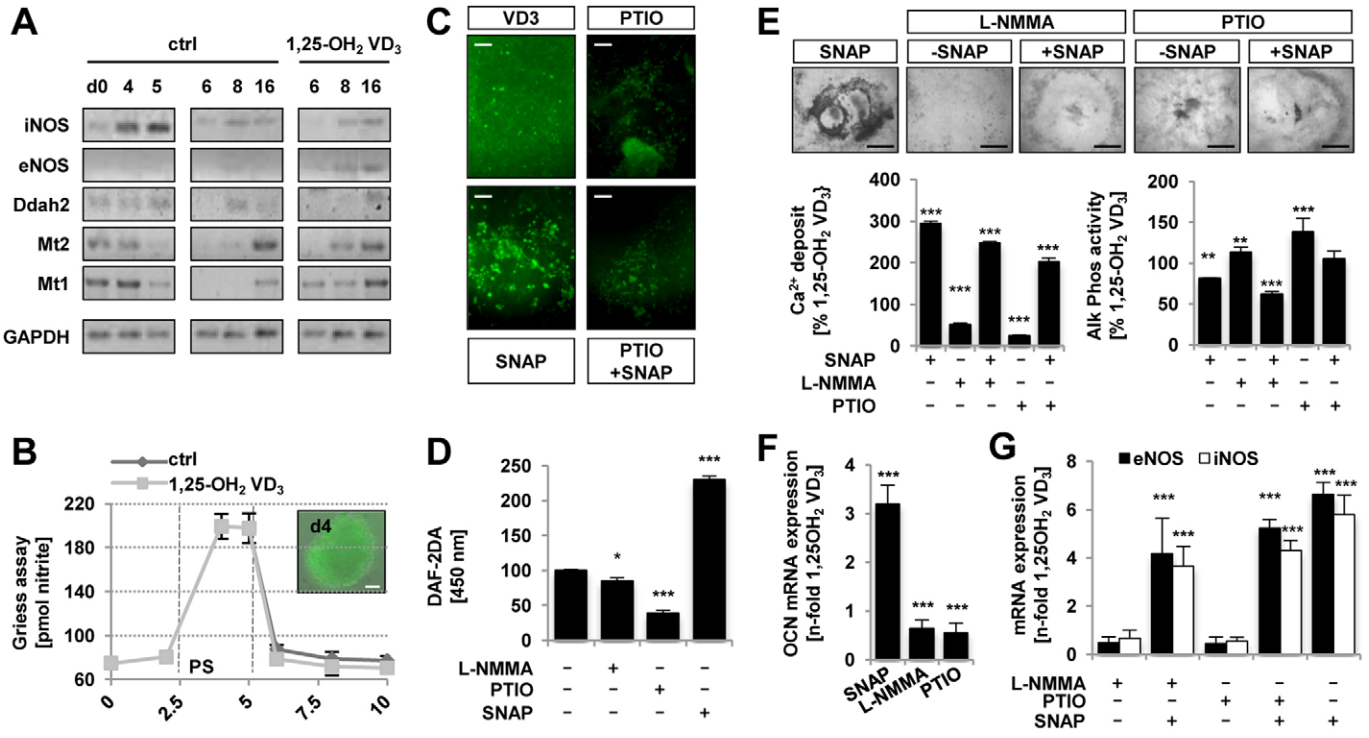

Fig. 1. ESCs respond to manipulation of NO levels with altered mineralization. (**A**) Transcripts for molecules involved in NO signaling can be detected by RT-PCR during early osteogenesis. mRNA expression levels vary between cultures that spontaneously differentiate (ctrl) and osteo-induced cultures (VD_3). (**B**) A Griess assay was performed to quantify levels of secreted NO in ESCs undergoing osteogenesis. PS indicates the differentiation stage previously associated with primitive-streak-like cells (Gadue et al., 2006). NO was also detected with DAF-2DA on differentiation day 4, which corresponds to the peak in NO generation (inset; scale bar: 50 μM). (**C–G**) ESCs were treated with NO donor SNAP and inhibitors L-NMMA or PTIO as indicated over the entire time in culture. (C) Cultures were incubated with DAF-2DA and fluorescing cells indicative of NO production were photographed. Scale bars: 100 μm. (D) DAF-2DA fluorescence was measured in cell lysates at 450 nm with a spectrophotometer, verifying inhibition or additional production of NO. (E) Culture calcification, visualized as a black deposit, is increased upon supplemented with NO. Increased calcium deposition and reduced Alk Phos enzyme activity (marker of preosteoblasts) in mature cultures (differentiation day 30) showed that increased NO concentration in the medium corresponds to an increase in osteogenesis. Scale bars: 100 μm. (F) Quantitative PCR for osteocalcin with standardization to glyceraldehyde 3-phosphate dehydrogenase (GAPDH; values are means ± s.d.; $n=3$), and normalization to cultures supplemented with VD_3 only (untreated). (G) Quantitative PCR for the eNOS and iNOS synthase mRNAs suggests a positive-feedback regulatory mechanism for NO signaling upon NO stimulation with SNAP. $^*P<0.1$, $^{**}P<0.01$, $^{***}P<0.001$ compared to untreated cultures [$1,25(OH)_2VD_3$ only].

observed in endothelial cells (Achan et al., 2002). Indeed, at differentiation day 4 and 5, Ddah2 and iNOS mRNA were regulated in tandem.

Two other mRNAs previously identified in our microarray were metallothioneins Mt1 and Mt2 (zur Nieden et al., 2007a). These metal binding proteins are an important component of intracellular redox signaling, including being a target for NO (Pearce et al., 2000; Casero et al., 2004). Within a cell, NO exposure may results in Mt mRNA elevation and Mt-based release of zinc (Katakai et al., 2001; St Croix et al., 2002). Mt1 and Mt2 expression was found concomitantly with iNOS expression, especially on day 4 of the differentiation and the later stages of differentiation.

Based on this observed mRNA regulation of iNOS, as an activator of NO synthesis, and Ddah2, as the degrading enzyme of the NO synthesis inhibitor ADMA, we expected to find elevated NO levels at around day 4 to 5 of the ESC differentiation. In the extracellular milieu, NO reacts with oxygen and water to form nitrates and nitrites, making it quantifiable using spectrophotometric assays. This feature was taken advantage of to measure the production of NO by ESCs in a time course experiment using the Griess assay. As expected, a sharp peak in cellular NO secretion was observed during early differentiation (Fig. 1B, day 4 of culture). The DAF-2AD fluorometric measure of intracellular NO also showed strong green fluorescence in developing 4-day-old embryoid bodies (Fig. 1B, inset).

Non-specific NOS inhibitors

Next, three consecutive ESC cultures were utilized for end point analysis (day 30 of the differentiation) to assess the impact of NOS inhibitors and/or NO supplementation on osteogenesis. The first experiment assessed the effect of adding the general NOS inhibitor, NG-monomethyl-L-arginine monoacetate (L-NMMA) together with a NO radical scavenger 2-phenyl-4,4,5,5-tetramethylimidazoline-1-oxyl 3-oxide (PTIO), or the exogenous NO donor S-nitroso-N-acetyl-penicillamine (SNAP) on VD_3-induced osteoblast differentiation. For each experiment, altered NO concentrations were confirmed by DAF-2DA quantitative analysis (Fig. 1C,D).

The effect of increased NO content on osteogenesis was confirmed by the increased presence of black appearing mineralized matrix (Fig. 1E, top panel) and quantitatively measured using the p-nitrophenol alkaline phosphatase (Alk Phos) assay, and the Arsenazo III calcium-binding dye. Mineralized calcium content dropped to approximately one half of the control level in the presence of NOS inhibitors, and was restored to twofold the basic VD_3 level using the NO donor in addition to the inhibitors (Fig. 1E). Threefold increases in mineralized calcium content, which occurred upon supplementation of cultures with SNAP alone, is consistent with the expectation that NO promotes osteogenesis. Alk Phos assay results showed a negative correlation to the calcium content: Alk Phos activity dropped with the addition of an NO donor in VD_3 media, and increased with NOS inhibition. As Alk Phos is a preosteoblast marker, maturing cultures as the ones assessed in this experiment will be characterized by lower activity levels of this enzyme. Our results therefore suggest that cultures treated with NO donor contained a higher number of mature osteoblasts, which have deposited more calcium into their extracellular matrix and have ceased to express Alk Phos.

Quantitative PCR of end point tissue cultures also showed an increase in the mRNA level of osteocalcin (OCN) in SNAP treated cultures, while the mRNA level for OCN were decreased upon NO synthase inhibition or NO scavenging, patterns that were congruent with the calcium content (Fig. 1F). Similarly, eNOS and iNOS gene transcripts in SNAP treated cultures (Fig. 1G) were increased, while mRNA for both enzymes remained similar to untreated controls in cultures that were treated with PTIO and L-NMMA. Since there was no appreciable difference in SNAP-induced upregulation of eNOS and iNOS mRNA, this data suggests a positive-feedback mechanism for the regulation of both synthase isoform mRNAs upon treatment with NO donor.

INOS- and eNOS-specific inhibition

A second ESC culture was then subjected to a further end point experiment involving the NOS inhibitors, diphenyleneiodonium (DPI) and L-N^5-(1-iminoethyl)ornithine (L-NIO), alone and in combination with the NO donor SNAP (Fig. 2A). Although both inhibitors can potentially act on both NOS isoforms, at the chosen concentration DPI was previously shown to preferentially inhibit iNOS (Stuehr et al., 1991; Wang et al., 1993; Dodd-o et al., 1997; Mendes et al., 2001), while L-NIO was shown to inhibit eNOS over iNOS (Rees et al., 1990; McCall et al., 1991). Our results showed that mineralized calcium content was nearly twofold

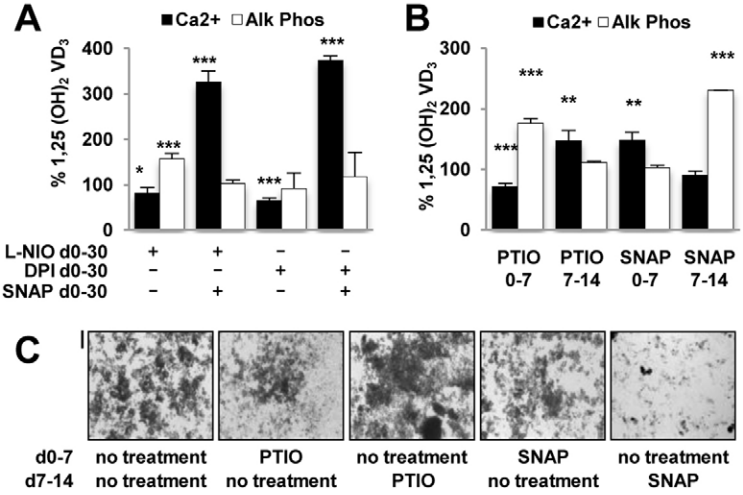

Fig. 2. eNOS and iNOS are involved in mineralization. (**A**) Calcium deposition and Alk Phos activity measured in mature cultures on day 30 upon treatment with L-NIO or DPI with or without SNAP (d0–30). (**B**) Amount of matrix-incorporated calcium and Alk Phos activity (d30) in cultures either supplemented with NO donor SNAP or NO scavenger PTIO in the first (d0–7) or second week (d7–14) of differentiation. (**C**) Day 30 morphology of cultures in B, supplemented with NO donor SNAP, NO scavenger PTIO or no additional treatment in the first or second week of differentiation. Scale bar: 100 μm. *$P<0.1$, **$P<0.01$, ***$P<0.001$ compared to $1,25(OH)_2VD_3$.

lower than VD_3 controls in the presence of iNOS inhibitor DPI. Calcium content was rescued in this treatment group with the addition of NO donor SNAP. While these results indicated a role for iNOS in calcium deposition, inhibition of eNOS by L-NIO did only lead to a slight decrease in calcium levels, an effect that was rescued with SNAP addition. In the Alk Phos assay, however, L-NIO treatment produced Alk Phos activity that was higher than VD_3 control levels, while Alk Phos activity was not significantly altered in the presence of DPI (with or without SNAP). Based upon these observations, we suggest that eNOS may affect Alk Phos activity, while iNOS may be involved in calcium deposition.

Split-phase inhibition of NO signaling

Based on the PCR data, which had implied specific regulation of endogenous eNOS and iNOS mRNA expression patterns, we then hypothesized that the first 2 weeks of the differentiation were specifically sensitive to alterations in NO concentrations. A third ESC end point protocol was then implemented to investigate the effect of split-developmental-phase supplementation. This included the addition of the NO scavenger PTIO or NO donor SNAP in the presence of VD_3 media during different phases of tissue culture, followed by analysis. Supplementation with SNAP and/or PTIO was conducted during early (day 0–7) and mid (day 7–14) phases of osteoblast differentiation, whereupon the efficiency of induction was observed by examining calcium content as well as Alk Phos activity (Fig. 2B) and culture morphology (Fig. 2C). The highest calcification accompanied by lower Alk Phos activity was noted in cultures that were supplemented with NO scavenger PTIO in week 1 and with SNAP in week 2, suggesting that osteogenesis may be supported by specific variations of NO levels during differentiation, in which higher NO levels in week 1 and lower NO levels in week 2 supported culture calcification and maturation.

iNOS overexpression induces a spontaneous loss of pluripotency

In order to characterize the osteogenic effects of the NO synthase isoforms in more detail, we next generated ESC lines that stably overexpressed the eNOS and iNOS isoform, respectively. Immediately after transfection and antibiotic selection, the iNOS-overexpressing ESCs lost colony morphology and started to grow as monolayer cultures (Fig. 3A). This could have not been caused by high density, as most of the cells in the dish were killed off by the antibiotic. The cells that survived were also highly migratory. When PTIO was added during transfection, the spontaneous loss of colony morphology was prevented (data not shown). In contrast, mock transfected ($[neo]^R$) and eNOS-overexpressing cells maintained normal ESC colony morphology. Intriguingly, when passaged with LIF, the $iNOS^+$ ESCs grew as single cells, but did not change morphology further, even after 50 passages. It appeared that the change in culture morphology in the $iNOS^+$ ESCs was accompanied by a reduction in Oct-4 and nanog mRNA and protein (Fig. 3B,C) as well as by an upregulation of T-Brachyury (T-Bra) and the osteoprogenitor-specific mRNAs for osterix and Cbfa1 (Fig. 3B).

iNOS overexpression accelerates osteogenic induction *in vitro* and *ex vivo*

Next, we aimed to examine the differentiation potential of the $iNOS^+$ ESCs and subjected them to a 30-day differentiation protocol comparing them to mock transfected and $eNOS^+$ ESCs. The typical black matrix was found in $[neo]^R$, eNOS ESCs and $iNOS^+$ ESCs. Moreover, all cultures were immunoreactive to osteocalcin and cadherin 11 antibodies (Fig. 3D, left panel), which are typically found in bone extracellular matrix and on osteoblasts. Furthermore, deposition of calcium was verified by von Kossa staining and incorporation of tetracycline (Fig. 3D, right panel).

As it, however, appeared from these histochemical analyses that calcification was enhanced in $iNOS^+$ ESCs over $eNOS^+$ and $[neo]^R$ ESCs, we next quantitatively determined the amount of calcium that was deposited by these different cell lines upon VD_3 induction. Already during early stages of differentiation (day 11), matrix calcium content in $iNOS^+$ ESCs was ~2.6-fold enhanced over $[neo]^R$ ESCs (Fig. 3E). By day 30, osteogenically differentiated $iNOS^+$ cultures also expressed higher levels of OCN ($2.7\pm0.5\times$), bone sialoprotein (BSP; $1.5\pm0.1\times$) and Cbfa1 ($16.25\pm2.9\times$) mRNAs than mock transfected differentiated cells, while mRNA expression of these genes was not significantly changed in $eNOS^+$ ESCs (Fig. 3F).

We also investigated the osteogenic potential of the $iNOS^+$ ESCs in bone explant co-cultures. Femurs were harvested from two months old mice, muscle and bone marrow were removed and bones cut into thin fragments. $iNOS^+$ ESCs were seeded onto bone fragments and were cultured for 30 days in osteogenic or control medium. Attachment of $iNOS^+$ ESCs to bone surfaces was controlled for by using q-dot-labeled cells. Compared to $iNOS^+$ ESCs differentiated in control medium only, $iNOS^+$ ESCs differentiated in bone slice co-cultures with control medium showed a 5-fold increase in OCN mRNA expression (Fig. 5G). The fold regulation was further increased to 20-fold by culturing $iNOS^+$ ESCs with bone fragments and osteogenic induction medium. Compared to osteogenically induced $iNOS^+$ ESCs without bone fragments, this represents a further enhancement of osteogenic yield by 1.4-fold. Similarly, BSP mRNA was enhanced in bone explant cultures (Fig. 5H). Coupled with our data from the inhibitor experiments, these results suggest that ESCs are particularly sensitive to changes in NO levels during early differentiation induction (week 1) and that undifferentiated ESCs respond to changes in NO levels with differentiation induction.

Stage-specific enhancement of osteogenesis through upregulation of NO

Based on our results we aimed to further refine the window of NO influence during week 1 of ESC differentiation in subsequent experiments. ESCs were treated with different combinations of the NO donor SNAP or NO scavenger PTIO during the first five differentiation days and supplemented with VD_3-containing osteogenic medium thereafter. Calcium deposition was measured as a readout for osteogenic yield and photomicrographs were taken after 30 days in culture (Fig. 4A). While the highest amount of deposited calcium was noted in cultures supplemented with SNAP from day 3 to 5, PTIO treatment in the same time window decreased calcium levels. When this treatment commenced just a day or two later (Fig. 4A, d4–5, d5–5) the effect was diminished. However, when NO levels were manipulated during days 0 to 3, the observed pattern was inversed to the point that we found lower levels of calcium deposition when cells were incubated with SNAP (days 0–3), and more efficient calcium incorporation when cells were treated with PTIO (days 0–3). Based upon these results, we concluded that ESC osteogenesis seemed to be elevated when NO levels were low between days 0 and 3, whereas NO levels must be

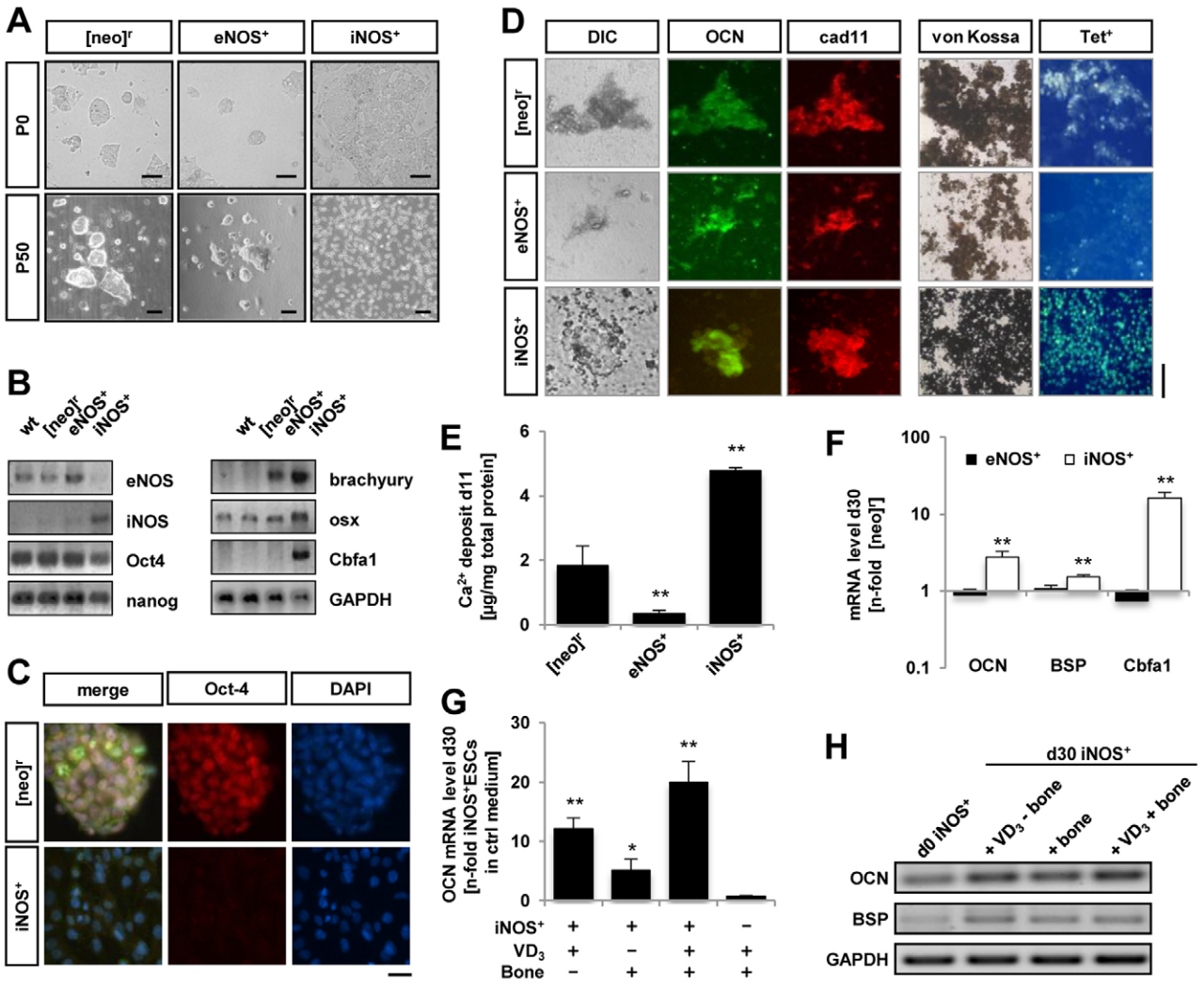

Fig. 3. Overexpression of iNOS causes spontaneous differentiation and accelerated osteogenesis. (**A**) Morphology of transfected ESCs after antibiotic selection and after 50 passages. Scale bars: 100 µm. (**B**) RT-PCR showing the respective overexpression of eNOS and iNOS mRNAs as well as the reduction of pluripotency markers and acquisition of lineage mRNA expression. (**C**) Immunocytochemistry with an anti-Oct-4 suggests a reduction in Oct-4 protein levels in iNOS$^+$ ESCs. Scale bar: 20 µm. (**D**) Immunocytochemical and histochemical analysis of osteogenically differentiated wild-type and NOS-overexpressing ESCs. Scale bar: 50 µm. (**E**) Calcium deposit in osteogenically differentiated cells as measured with Arsenazo III on day 11. Values are means ± s.d.; n=5. (**F**) Quantitative PCR showed enhanced expression of bone-specific mRNAs in iNOS$^+$ cells. N-fold regulation over mock transfected cells was calculated according to the $\Delta\Delta C_T$ method; values are means ± s.d.; n=3. (**G**) iNOS-overexpressing cells were differentiated on explanted bone chips and harvested for quantitative PCR after 30 days in culture. N-fold regulation over undifferentiated iNOS$^+$ ESCs was calculated as for F. (**H**) RT-PCR for bone mRNA expression on bone explant cultures. *P<0.1, **P<0.05. cad11, cadherin 11; DIC, differential interference contrast; osx, osterix; Tet$^+$, tetracycline-positive cells.

elevated between days 3 and 5 in order for osteogenesis to occur effectively.

Upstream NO effectors

In the vasculature, insulin and acetylcholine (ACh) regulate the release of NO (Förstermann and Neufang, 1984; Zeng and Quon, 1996) and the regulation of mRNA expression of constitutive eNOS (Papapetropoulos et al., 1999; Kuboki et al., 2000). To verify that the effects on osteogenesis were truly based on generation of NO, we conducted another experimental set, in which we treated ESCs with these two upstream NO regulators during days 3 to 5. Prior to the experiment, the increase in NO secretion caused by ACh and insulin was validated with the DAF-2DA assay as described above and was found to be concentration dependent (data not shown). Calcium levels in mature cultures (day 30) were measured upon treatment with ACh and insulin (during days 3 to 5) and compared to levels found in non-treated osteogenic cultures. While PTIO effectively decreased calcium deposition as also observed in the previous experimental sets, SNAP, ACh and insulin increased calcium levels (Fig. 4B). From these experiments we were able to conclude that both ACh and insulin showed a similar outcome as SNAP supplementation.

NO enhances osteogenesis through regulation of ESC differentiation stages that are equivalent to primitive streak formation

Fehling et al. had previously shown that transcripts for T-Bra appear around the time window that was responsive to elevated NO in our study (days 3–5) (Fehling et al., 2003). *In vivo*, T-Bra expression marks a population of cells in the primitive streak (PS)

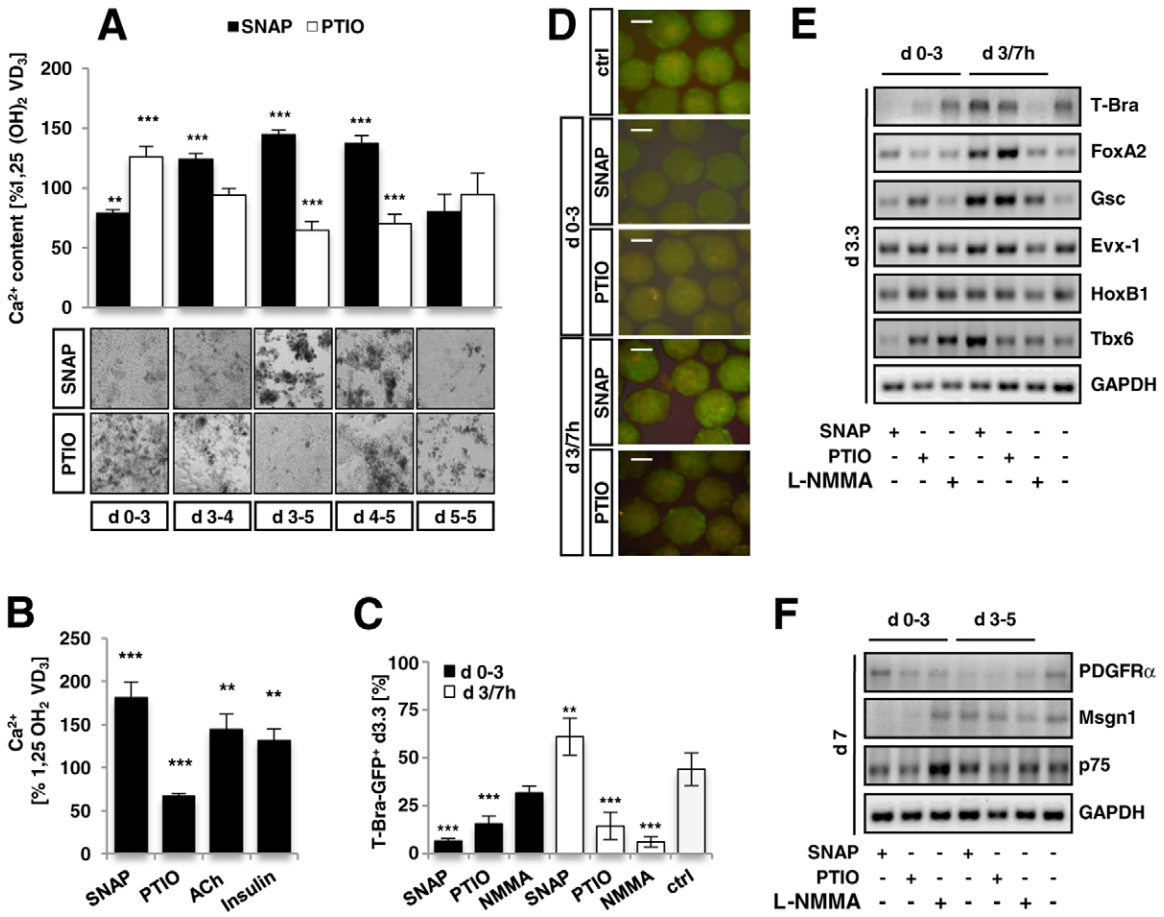

Fig. 4. NO augments osteogenesis through regulation of T-Brachyury. ESCs were treated with NO donor SNAP (100 μM) or NO scavenger PTIO (100 μM) during the first five days of differentiation as indicated and supplemented with VD_3 containing osteoinducing medium thereafter. (**A**) Deposition of calcium was measured and photomicrographs were taken after 30 days in culture. Higher calcification was seen when NO levels were elevated by SNAP and when NO levels were dampened with PTIO between days 0 and 3. $^{**}P<0.01$, $^{***}P<0.001$ compared to $1,25(OH)_2VD_3$. (**B**) Deposited calcium in cultures supplemented with acetylcholine (Ach; 2 μM) and insulin (1 μg/ml), which are known stimulators of NO secretion. $^{**}P<0.01$, $^{***}P<0.001$ compared to $1,25(OH)_2VD_3$. (**C**) T-Bra–GFP ESCs were cultured for 3 days and treated with SNAP, PTIO or NMMA either for the whole time or on day 3 for 7 hours. Flow cytometric quantification of GFP^+ cells on day 3.3 relative to non-treated controls. (**D**) Fluorescence microscopy was performed on embryoid bodies generated from T-Bra–GFP ESCs on differentiation day 3.3. Scale bars: 200 μm. (**E**,**F**) RNA was harvested on day 3.3 (E) and day 7 (F) for RT-PCR analysis of expression of genes associated with early development. Ctrl, control; FoxA2, forkhead box A2; Gsc, goosecoid; Evx-1, even-skipped homeobox 1; HoxB1, homeobox B1; Tbx-6, T-box 6; PDGFRα, platelet-derived growth factor receptor; Msgn1, mesogenin1.

that participates in gastrulation events. As this process is modeled during ESC differentiation (Gadue et al., 2006), we sought to investigate a role for NO in the specification of PS-like cells. We therefore examined the expression pattern of T-Bra on day 3.3 of differentiation while manipulating NO levels between days 0 and 3 and on day 3 for 7 hours just prior to cell harvest. This is a time point of differentiation that we had found to correspond to a peak expression in T-Bra in our cultures (data not shown) and that had also been described by Gadue et al. (days 2.5–5 in their study) (Gadue et al., 2006). Specifically, since calcium deposition was enhanced by PTIO treatment from day 0 to 3 (low NO levels), we expected to detect enhanced T-Bra expression in cultures with NO inhibition from day 0 to 3. Similarly, since calcium deposition was enhanced by SNAP treatment (high NO levels) between days 3 and 5, we expected to find higher T-Bra expression also in cultures with enhanced NO levels on day 3.

Using embryoid bodies (EBs) generated from ESCs that were stably transfected with a T-Bra–GFP reporter, however, the highest induction of T-Bra-positive cells and mRNA was registered when NO levels were elevated with SNAP on day 3 for 7 hours, while we found a very low level of T-Bra protein and mRNA expression under SNAP donor treatment, when treatment commenced on day 0 of the differentiation (Fig. 4C,D). Also congruent with the calcium assays, cultures in which NO production was inhibited with PTIO and L-NMMA between days 3 and 5 clearly showed significantly lower levels of T-Bra protein (as per GFP-positive cells) and message (Fig. 4C,E). However, we did not note the expected increase in fluorescence when NOS was inhibited with PTIO between days 0 and 3, but instead noted a decrease (Fig. 4C,D). These results led us to conclude that the increased calcification seen in SNAP-treated cultures (days 3–5), the decrease of calcification in SNAP-treated cultures (days 0–3) and the decrease in calcification following PTIO treatment (days 3–5) fully correlated with the regulation of T-Bra during early differentiation. However, the observed increase in calcification upon PTIO supplementation on days 0

to 3 did not correlate with its regulation of T-Bra and therefore may be attributed to other effects.

Wishing to elucidate the consequences of T-Bra regulation on further ESC commitment, we subsequently examined the expression of FoxA2, Gsc and evx-1, which are found in the anterior primitive streak during gastrulation (Hallonet et al., 2002; Blum et al., 1992; Nakanishi et al., 2009; Dush and Martin, 1992), as well as HoxB1 and Tbx6, which are found in the posterior primitive streak (Forlani et al., 2003; Chapman and Papaioannou, 1998) (Fig. 4E). Based on the effects of NO donor and inhibitors on osteogenesis that we had detected and the role of these genes in early embryonic development, which leads to the specification of cells with osteoprogenitor potential, we expected to find an upregulated expression of all genes upon SNAP supplementation on day 3 (which upregulated calcium content), and a downregulation of expression upon SNAP treatment between days 0 and 3. While expression of most of these markers was indeed lower in cells that received SNAP between days 0 and 3, it was higher in cells that received SNAP on day 3 (Fig. 4E), supporting our hypothesis. Based on the calcium content in mature cultures, the opposite pattern was expected for L-NMMA and PTIO, however, was only verifiable in cells treated on day 3. Similar to the regulation of T-Bra mRNA expression, inhibition of NO between days 0 and 3 by PTIO or L-NMMA did not lead to downregulation of these primitive streak associated messages.

Since osteoblasts may be specified from a neural crest or a mesodermal origin, we also investigated the expression pattern of Mesogenin (Msgn1), a gene that controls presomitic mesoderm maturation downstream of T-Bra (Wittler et al., 2007), as well as the paraxial mesoderm associated gene PDGFRα (Orr-Urtreger et al., 1992; Takakura et al., 1997) and the neural crest marker/mesenchymal stem cell associated marker p75 (Jiang et al., 2009) a few days further into the differentiation (Fig. 4F). Of these, Msgn1 was upregulated by SNAP treatment on days 3–5 and downregulated by SNAP treatment on days 0–3. PDGFRα message, in contrast, was downregulated by SNAP supplementation on days 3–5 and upregulated when treatment commenced on day 0.

In summary, the differences in responsiveness to NO at both developmental stages (day 3.3 and day 7) were readily apparent in cells treated with NO modulators on day 3, where they clearly indicated a positive relationship between high NO levels and T-bra expression and thus development of PS-like cells in ESCs and a negative relationship between low NO levels and T-Bra expression. The decreased calcification noted when NO levels were increased between days 0 and 3 also fully correlated with the development of a T-Bra^{+} population and further progenitor commitment. However, the relationship between low NO levels during the first 3 days of differentiation and T-Bra regulation could not be confirmed.

NO enhances osteogenesis through activation of CatnB

We have previously shown that the levels of nuclear CatnB play an important role during the matrix maturation and calcium mineralization phases of the osteogenic specification path in ESCs (zur Nieden et al., 2007a; Davis and zur Nieden, 2008). Since T-Bra had been described as a transcriptional target for CatnB (Arnold et al., 2000), we set up another set of experiments aiming to elucidate the relationship between NO and CatnB during PS formation in ESCs. Using a LEF/TCF–GFP reporter ESC line, we were able to show that nuclear CatnB indeed seemed to be endogenously active at around the time of the primitive streak equivalent (Fig. 5A, d2.5–5). As NO has previously been shown to induce CatnB (Shtutman et al., 1999), we sought to investigate whether the NO effect might be manifested at the level of CatnB and whether CatnB might itself be involved in PS specification.

Next, we investigated whether expression levels for CatnB mRNA were proportionally modulated by NO in the first three differentiation days. We found extremely low CatnB mRNA levels detectable in SNAP day 0–3 cultures, while SNAP when given on day 3 for 7 h showed equal levels of CatnB mRNA expression compared to control (untreated) levels (Fig. 5B). However, the expected pattern in day 0–3 NO-inhibited cultures were again not clear.

We also observed that treatment with LiCl, which artificially elevates nuclear CatnB levels in cells by inhibiting GSK-3β, which normally tags CatnB for degradation (van Noort et al., 2002), increased calcium deposition and decreased Alk Phos activity in ESC cultures when treatment fell between days 3 and 5 of the differentiation (Fig. 5C). In contrast, LiCl treatment during days 0 to 3 decreased cellular calcification and increased Alk Phos activity. This result seems congruent with a role for CatnB in early differentiation. The fact that the effects caused by differentiation-stage-dependent CatnB elevation mimicked the SNAP effect seen earlier (see Fig. 4A) led us to investigate whether there was a closer link between CatnB and NO levels.

Since CatnB is heavily regulated at the protein level and its localization largely dictates cell fate (Moon et al., 2002), we then used the LEF/TCF–GFP reporter ESC line to evaluate CatnB activity in the nucleus. Total levels of CatnB mRNA expression were compared to GFP mRNA expression levels by quantitative PCR, where reporter GFP activity was used as a read-out for nuclear LEF/TCF activation (Fig. 5D). Manipulation of NO levels with NO donor, scavenger or NOS inhibitor between days 3 and 5 seemed to alter the ratio between total cellular CatnB and nuclear CatnB. While SNAP treatment did not significantly alter the levels of total cellular CatnB, a specific increase in GFP expression representative of the nuclear CatnB activity was observed (2.1-fold, $P<0.001$). In contrast, both NOS inhibition and NO scavenging, led to a marked decrease in GFP expression ($P<0.001$). Since the reporter cell line only allows conclusions about the expression of the CatnB cofactor LEF/TCF and therefore only indirectly quantifies CatnB transcriptional activity, we next also evaluated whether stabilization of CatnB protein occurred upon treatment with NO donor SNAP or NO scavenger PTIO. Western blot analysis on fractionated protein lysates showed that SNAP treatment on day 3 for 7 hours led to stabilization of CatnB, while treatment with PTIO at the same time had the opposite effect (Fig. 5E).

Taken together, we were able to confirm that NO signaling needed to be activated on day 3 of the ESC differentiation to regulate T-Bra and CatnB, and that inhibition of NO signaling at that time of differentiation decreased T-Bra and CatnB. In contrast, NO activation through SNAP between days 0 and 3 inhibited T-Bra expression and CatnB nuclear function. However, the effects of the NO inhibitors L-NMMA and PTIO during initial differentiation (days 0–3) were less clear. Therefore, the TopFlash/FopFlash system was employed to test the relationship between NO modulators and LEF/TCF activation

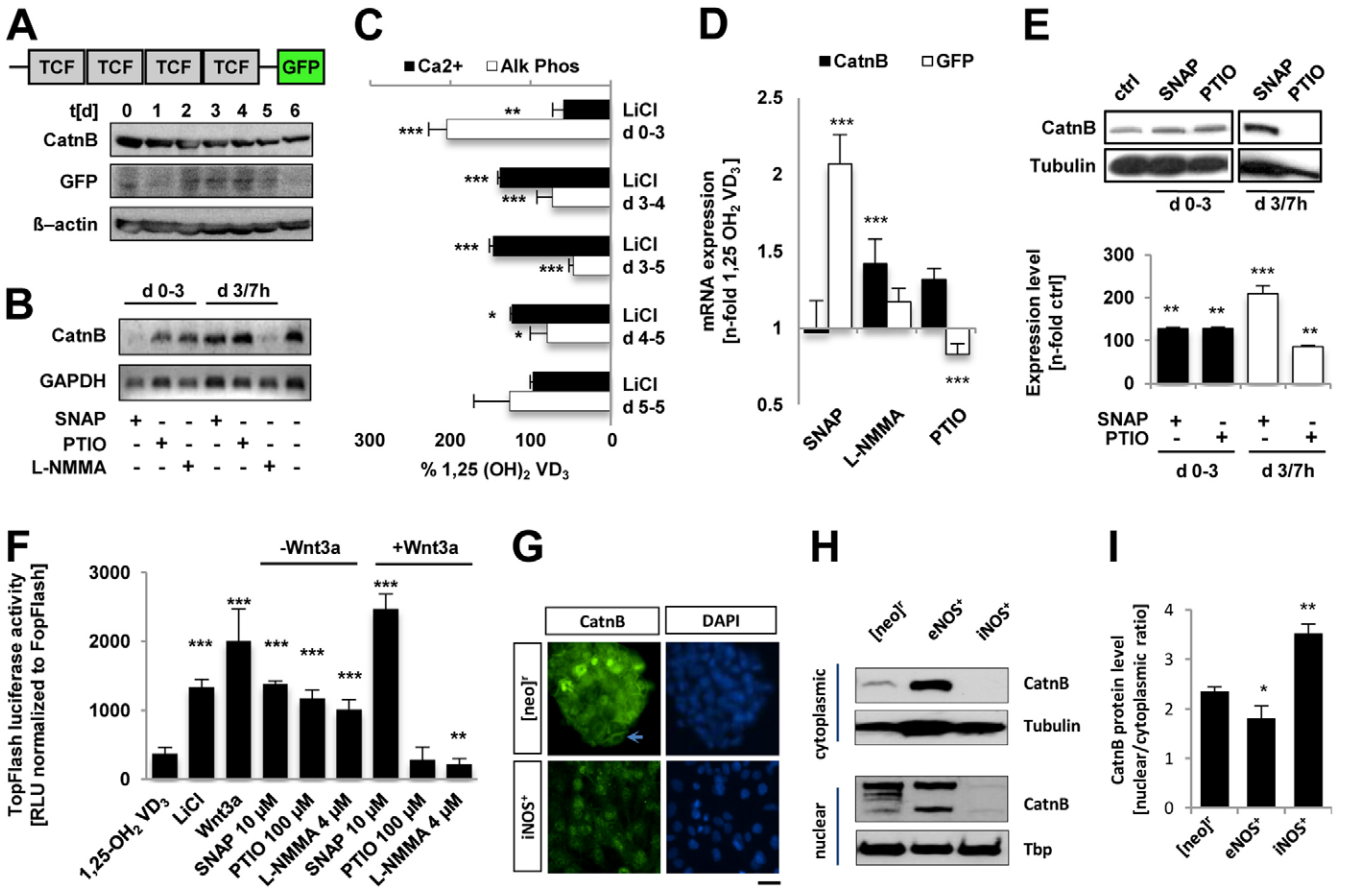

Fig. 5. NO modulates CatnB levels. (**A**) Protein lysates from LEF/TCF–GFP ESCs were analyzed by western blotting for total CatnB protein and LEF/TCF reporter activation. The GFP signal is enhanced during specification of the primitive streak (d2.5–5). (**B**) ESCs were cultured for 3 days and treated as indicated, then assayed for mRNA expression levels of CatnB on day 3.3. (**C**) ESCs were treated with LiCl (20 mM) during the first 5 days of differentiation as indicated and supplemented with VD_3 containing osteoinducing medium thereafter. Deposition of calcium and Alk Phos activity levels were measured after 30 days in culture. LiCl supplementation mimicked the SNAP effect since LiCl given between days 3 and 5 enhanced calcium deposition whereas LiCl supplementation during days 0–3 decreased calcium deposition. (**D**) The LEF/TCF–GFP reporter ESC line was treated with SNAP, L-NMMA or PTIO on day 3 of differentiation for 7 hours and cells were harvested for RNA isolation. Total levels of CatnB were measured by quantitative PCR and GFP expression levels were examined as a measure for nuclear CatnB/LEF/TCF activity. Expression levels were normalized to GAPDH and standardized to non-treated cultures. Values are means ± s.d.; $n=3$. (**E**) Cytoplasmic protein lysates from day 3.3 differentiating EBs were assayed for stabilized CatnB content by western blotting. Protein expression levels in blots were measured by densitometry (bottom graph); $n=3$ blots. A representative blot is shown in the top panel. (**F**) HEK293T cells were transfected with 500 ng of either TOPFLASH or FOPFLASH. 24 h after transfection, the cells were treated with NO modulators. 24 h after treatment initiation, cells were lysed and relative light units were determined. Reporter activity in TOPFLASH-transfected cells relative to the FOPFLASH response is shown. Values are means ± s.d. from three independent experiments. $^{**}P<0.01$, $^{***}P<0.001$ compared to untreated cultures. (**G**) Immunocytochemistry with an anti-CatnB antibody suggests a loss of the membrane-specific CatnB pool (arrow in $[neo]^r$) in $iNOS^+$ ESCs, and all the CatnB that is present primarily resides in the nucleus. Scale bar: 20 µm. (**H**) Western blot on fractionated protein lysates from mock transfected ($[neo]^r$), $eNOS^+$ and $iNOS^+$ ESCs. (**I**) Calculated nuclear to cytoplasmic CatnB ratio from densitometry data performed on three independent western blots. Tbp, TATA binding protein.

in HEK293T cells (Fig. 5F). As expected and seen in ESCs, SNAP increased luciferase levels, suggesting the activation of LEF/TCF-CatnB mediated transcription upon SNAP treatment. Interestingly, the inhibitory effect of PTIO and L-NMMA on LEF/TCF activation was hardly evident in these HEK293T cells. Only when canonical Wnt signaling was activated with recombinant Wnt3a protein (50 ng/ml), both L-NMMA and PTIO decreased LEF/TCF activation. This finding may explain the previously noted controversial effects in ESCs under NO inhibitor treatment between days 0 and 3 and suggests that L-NMMA and PTIO are only potent in decreasing CatnB/LEF/TCF nuclear activity when Wnt signaling is in an activated state. In contrast, SNAP may elevate CatnB levels in cells that have either inactive or active Wnt signaling.

After having confirmed a role for NO in the regulation of CatnB nuclear activity, we next determined CatnB activation levels in the $iNOS^+$ ESCs. Simultaneously with the reduction in Oct-4 expression (see Fig. 3), we observed a loss of membrane bound CatnB (Fig. 5G), which is typically found in undifferentiated ESCs (Lyashenko et al., 2011). Instead, CatnB was found to be nuclear in $iNOS^+$ ESCs, although overall levels seemed to be lower than in mock transfected or $eNOS^+$ ESCs (Fig. 5H). When the ratio between cytoplasmic and nuclear CatnB was calculated from the densitometric western signals, we found that the $iNOS^+$ ESCs had the highest nuclear to cytoplasmic CatnB ratio of all cell lines examined (Fig. 5I). Therefore, also in $iNOS^+$ ESCs, we were able to identify a correlation between differentiation induction, T-Bra expression and nuclear CatnB activity.

LiCl treatment at the time of PS formation enhances osteogenesis in human ESCs

Similarly to the results found with murine ESCs, we were able show that the role of CatnB in the specification of PS-like cells and subsequent osteogenic commitment was transferable between species. In order to proof responsiveness of human ESCs to CatnB levels, the human ESC line CA-1 was supplemented with LiCl from days 3 to 5 and then further differentiated with VD_3 from day 5 onwards (Fig. 6). This treatment regimen was compared to the widely used osteogenic induction protocol using dexamethasone between differentiation days 7–14 (Bielby et al., 2004) and VD_3 only. As expected, elevation of CatnB through LiCl at the time of PS specification also increased the amount of calcium deposited by mature CA-1 hESC-derived osteoblasts compared to VD_3 only and also compared to dexamethasone, indicating that human ESCs as well are capable of responding to elevated CatnB levels with an enhanced osteogenic differentiation yield.

NO and elevated CatnB modulate cGMP levels during PS formation

We further determined the effect of NO on intracellular levels of cGMP, a proven down-stream target of NO (Fig. 7A). Cyclic GMP levels were significantly higher (123.2% and 126.3%) in cultures that were treated with SNAP on days 3–5, allowing for the conclusion that high amounts of cGMP are beneficial for the development of PS-like cells at the time of T-Bra expression. Interestingly, NOS inhibition and NO scavenging by PTIO and L-NMMA did not significantly alter cGMP levels in ESCs. However, treatment with BIO, a pharmaceutical inhibitor of GSK-3β, had a similar effect to that observed with SNAP as it also elevated cGMP (142.5±5.2%, $P<0.001$). The corresponding non-active MeBIO did not show alterations in cGMP levels, again underlining the fact that the SNAP effect may be mediated by CatnB levels.

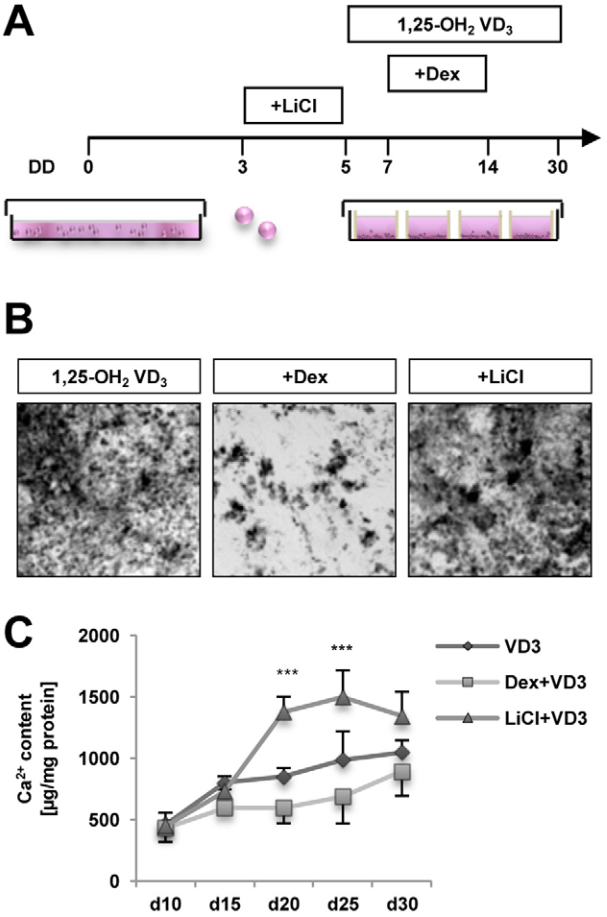

Fig. 6. LiCl enhances osteogenic differentiation in human ESCs when administered during PS formation. (**A**) Overview of experimental set-up. The human ESC line CA-1 was differentiated with VD_3 and supplemented with dexamethasone between differentiation days 7 and 14 or LiCl from days 3 to 5. (**B**,**C**) Elevation of CatnB through LiCl at the time of PS formation increased the amount of mineralization (B) and calcium deposited (C) by mature CA-1 hESC-derived osteogenic cultures compared to VD_3 only. ***$P<0.001$ compared to cultures treated with $1,25(OH)_2$ VD_3. Dex, dexamethasone.

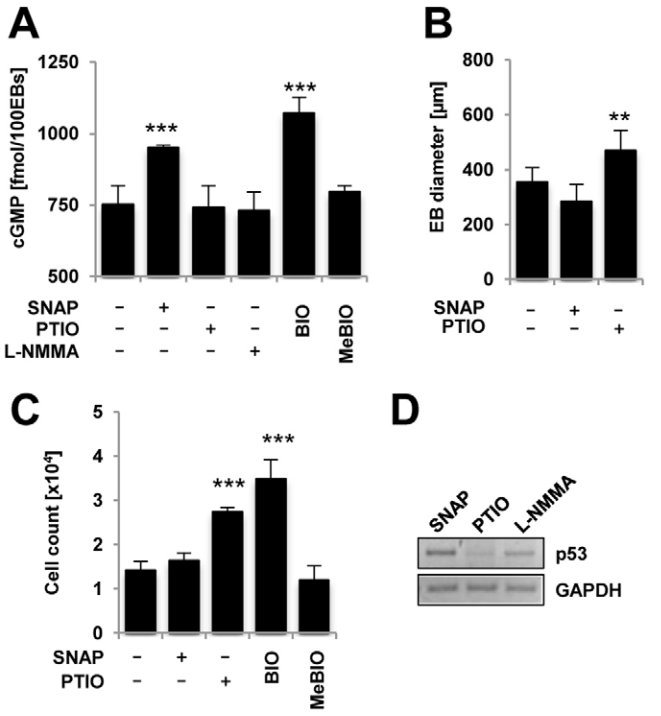

Fig. 7. NO selectively modulates cGMP levels and regulates cell growth in EBs. ESCs were induced to form EBs in hanging drops (3.75×10^4/ml) and supplemented with SNAP (100 µM), L-NMMA (4 µM) or PTIO (100 µM) between differentiation days 3 and 5. (**A**) Cyclic GMP levels were measured in ESCs treated with NO donors or inhibitors. Elevated NO levels increased cGMP production, whereas inhibition of NO did not alter cGMP levels. Manipulation of CatnB levels with BIO (2 µM), a small molecule inhibitor of GSK-3β, leading to elevated nuclear CatnB activity, and also increased cGMP similar to SNAP. The kinase-inactive analog 1-methyl-6-bromoindirubin-3′-oxime (MeBIO) served as a control and showed no influence on cGMP levels. (**B**) EB diameters were determined with the Nikon Elements software from photomicrographs (75 EBs were measured in each group). (**C**) Cell counts of 250 EBs were taken on day 5. Decreasing NO levels with the NO scavenger PTIO increased the number of cells. (**D**) Expression levels of p53 in treatment groups were assessed by semi-quantitative RT-PCR with GAPDH as the housekeeping gene. ***$P<0.001$ compared to untreated controls. BIO, 6-bromoindirubin-3′-oxime; cGMP, cyclic guanosine monophosphate; MeBIO, methyl-BIO (inactive).

NO controls cell number and p53 mRNA expression

To assess the effect of NO on the growth of ESCs during early differentiation, EB size and cell number was documented (Fig. 7B,C). SNAP treatment had no significant effect on the growth of ESCs neither when evaluated through EB diameter nor through counting the number of cells per EB. In contrast, PTIO treatment from day 0 to day 3 increased the number of cells in each EB to 338% and EB size to 147%.

We also examined the hypothetical connection between NO regulated cell growth and CatnB, by supplementing ESCs with BIO. The results observed indicated that such stabilized CatnB levels also led to an increase in EB cell number mimicking the effect seen with the NO scavenger, not the NO donor (Fig. 7B,C). Growth furtherance in PTIO treated EBs was correlated with decreased p53 mRNA expression (Fig. 7D).

Discussion

Our results support the finding of other studies showing that nitric oxide (NO) is involved in osteogenesis. This is illustrated by threefold increases in mineralized calcium content upon NO supplementation of cultures. In addition, our findings further show that the NO effects we observed in osteoblast differentiation are restricted to particular phases of development.

Specifically, we have observed that NO modulates osteogenesis through the regulation of PS formation and through Wnt/CatnB signaling whereby the activation state of the Wnt pathway seems to regulate the exact response to NO. Our observations that: (1) higher levels of the early pan-mesodermal marker T-Bra and posterior PS markers were expressed in response to NO supplementation at key early points in differentiation; (2) T-Bra-GFP-transfected cells displayed an increase in fluorescence during the same time points; and (3) NO increased LEF/TCF activity in Wnt3a-induced HEK293 cells provide evidence for this conclusion. Furthermore, LiCl and BIO supplementation, which have been shown to increase CatnB activity temporally, mimicked the effect of NO supplementation. While crosstalking to the Wnt/CatnB signaling pathway, higher NO levels seem to be involved in early fate decisions of ESCs.

The dependency of T-Bra expression on activated Wnt/CatnB signaling was first described a few years ago (Yamaguchi et al., 1999; Arnold et al., 2000). Mice that lack CatnB manifest a defect in anteroposterior axis formation at E5.5, do not form mesoderm or head structures, and show pronounced apoptosis at the time of death, which occurs at approximately E7.5 (Huelsken et al., 2000). Of the various upstream Wnt effectors, Wnt3 is expressed earliest during development, its expression being apparent immediately before gastrulation (E6.25) in the proximal epiblast of the egg cylinder (Liu et al., 1999). *Wnt3*$^{-/-}$ mice develop a normal egg cylinder, but do not form a primitive streak, mesoderm, or node.

While NO has been reported to control T-Bra levels in ESCs recently (Spallotta et al., 2010), we show here for the first time that NO potentially crosstalks with Wnt/CatnB signaling during primitive streak formation in ESCs to regulate T-Bra. Previous studies have speculated that this NO/Wnt crosstalk plays a role in colon cancer, leukemia, and colitis (Williams et al., 2003; Nath et al., 2005; Wang et al., 2009). In contrast to our findings, these reports put forward the hypothesis that NO downregulates CatnB and iNOS. However, we believe that the discrepancy seen between these and our study is based on the fact that the Wnt activation state of ESCs may be different to that of cancer cells. This is a likely hypothesis, since cancer cells often show mutations in a wide variety of molecules associated with the Wnt signaling pathway, including CatnB itself (Moon et al., 2002).

Recently, Du and colleagues have identified two TCF4 binding elements in the human iNOS promoter, which could explain the feedback observed on iNOS mRNA expression following NO treatment in ESCs. In addition, negative feedback via CatnB/TCF may also be possible (Du et al., 2006). Du et al. also proposed that LiCl enhances iNOS expression and NO production by regulating CatnB (Du et al., 2006).

Whereas the regulation of the iNOS promoter through CatnB is well established, little is known about a possible mechanism of how NO regulates CatnB. Taken all our data together, we are not able to state that a direct interaction between NO and CatnB exists, rather our studies suggest a correlative effect of NO on Wnt/CatnB. An indirect crosstalk could for example be possible through NO regulation of CatnB transcription. For example, NO is known to activate the transcription factors E2F1, NFKB, AP1, AP2, CREB, and SP1 (Sellak et al., 2002; Cui et al., 2005; Dhakshinamoorthy et al., 2007; Seo et al., 2008). When we bioinformatically examined the CatnB promoter for binding sites of these NO-induced transcription factors, we found that all of the mentioned transcription factors could potentially regulate CatnB mRNA expression, since all of these have binding sites on the CatnB promoter (Li et al., 2004).

Similarly, ACh and insulin, which were used as upstream NO regulators in this study, because they are known to cause increases in NO levels (Zeng and Quon, 1996; Kuboki et al., 2000; Zecchin et al., 2007), may indirectly affect CatnB through generation of NO. However, they may also directly affect the CatnB protein through interaction with their respective activated receptors. As Salmanian and colleagues have shown, expression of the M3-muscarinic acetylcholine receptor and subsequent activation of Gαq might stabilize CatnB protein via inhibition of GSK-3β (Salmanian et al., 2010). Insulin receptor activation may in turn stimulate phosphotidylinositide 3-kinase (PI3K) activity (reviewed by Cheng et al., 2010). Phosphatidylinositol 3,4,5-trisphosphate produced by PI3K recruits the Ser/Thr kinase Akt to the plasma membrane, and Akt can phosphorylate several substrates relevant to insulin-like signaling, among them GSK-3β (Fukumoto et al., 2001). This phosphorylation of GSK-3β inactivates its capability to phosphorylate CatnB at Ser33/37, thereby reducing the amount of CatnB that is tagged for proteasomal degradation. Ultimately, insulin receptor activation may thereby increase the amount of stabilized cytoplasmic CatnB, which is then available for shuttling into the nucleus.

Our results further suggest that NO may have an effect on either ESC proliferation or apoptosis, as we have noted changes in EB sizes and cell number. A conceivable link between NO and changes in cell number lies in the known interactions of NO or CatnB with p53 and cell cycle regulatory genes. For example, in rabbit articular chondrocytes, human tumor cells lines and mouse fibroblasts exposure to NO stimulated p53 mRNA expression (Forrester et al., 1996; Wang et al., 2007). Additional studies suggest that overexpression of CatnB also results in accumulation of p53, whereas overexpression of p53 leads to a downregulation of CatnB (Damalas et al., 1999; Sadot et al., 2001). Cross talk between Wnt signaling and the p53 signaling pathway has thus been described as a link between Wnt signaling and apoptosis. In contrast, WISP-1 (Wnt-1-induced secreted protein), a target of Wnt/CatnB signaling, has been shown to activate the anti-apoptotic signaling pathway

mediated by Akt, to prevent cells from undergoing p53-dependent apoptosis (Su et al., 2002).

We also showed that NO is exerting its effects in ESCs through cGMP. There is increasing evidence that cGMP can play an important role in cellular proliferation, differentiation, and apoptosis (Shimojo et al., 1999; Loweth et al., 1997; Chiche et al., 1998). The rate of its synthesis is regulated by guanylyl cyclases, which are activated by NO (Stacey et al., 1998). Having several intracellular targets, NO can bind to specific phosphodiesterases, which normally degrade cGMP (Smolenski et al., 1998) and it can also activate cGMP-gated cation channels, protein kinase G and protein kinase A (Lincoln and Cornwell, 1993).

We conclude that during ESC osteogenesis, NO levels fluctuate with the stage of differentiation. Furthermore, NO seems to act as a modulator of PS formation, and regulator of cell growth in a subset of cells by either directly or indirectly manipulating CatnB nuclear activity.

Materials and Methods

Tissue culture

All medium components were purchased from Invitrogen (Carlsbad, CA, USA). Mouse embryoid bodies were formed from the D3 ESC line (ATCC) using the previously described, but modified hanging drop method (Wobus et al., 1991; Trettner et al., 2011). Human ESC colonies from the CA-1 line (Adewumi et al., 2007) were separated from their feeder layer with dispase (1 mg/ml), resuspended in murine ESC medium and transferred to low attachment dishes (Costar) for spontaneous formation of EBs. Osteogenic differentiation was supported through the addition of β-glycerophosphate [10 mM], ascorbic acid [50 μg/ml] and 5×10^{-8} M 1α,25-$(OH)_2$ vitamin D_3 as described for murine differentiations (zur Nieden et al., 2003). Dexamethasone (5 nM) was substituted for VD_3 in human ESC cultures as indicated. Media and all additional supplements were replaced every second day.

NOS inhibitors included the general inhibitor L-NMMA (NG-monomethyl-L-arginine monoacetate; 4 μM), the more specific iNOS inhibitor, flavoprotein binder DPI (diphenyleneiodonium; 50 nM) (Stuehr et al., 1991; Mendes et al., 2001) and the eNOS inhibitor L-N^5-(1-iminoethyl)ornithine, dihydrochloride (L-NIO; 1 μM) (Rees et al., 1990; McCall et al., 1991). In addition, PTIO (2-phenyl-4,4,5,5-tetramethylimidazoline-1-oxyl 3-oxide; 100 μM] was used as a nitric oxide scavenger, while SNAP (S-nitroso-N-acetyl-penicillamine; 100 μM), was used as an exogenous NO donor (Ignarro et al., 1981). Concentrations were as indicated here, unless otherwise noted.

Plasmids and stable expression in ESCs

A murine D3 ESC line carrying a GFP reporter under the control of 4 LEF/TCF binding sites was kindly provided by Dr Irving Weismann (Stanford University) and has been used previously (zur Nieden et al., 2007a). In order to build a GFP expression plasmid under the control of the murine T-Brachyury promoter, the promoter sequence was amplified by PCR (primer sequences: 5′-CTTCACGCCAGAGGTTAAAC-3′ and 5′-ACCTTCCAGGAGTCTTGACT-3′) from ESC genomic DNA and subcloned into the *Xho*I and *Eco*RI sites of pEGFP-1 (Clontech).

The murine inducible nitric oxide synthase cytomegalovirus promoter construct (piNOSL8) was obtained from Oxford Biomedical Research (cat. no. NS05). The 3934 bp *Hin*dIII–*Eco*RV fragment from piNOSL8 was inserted into the *Hin*dIII–*Eco*RV site of pcDNA3.1 (Invitrogen) to yield piNOS3.1. The human eNOS cDNA plasmid PM831221 was obtained from Dr Philip A. Marsden (University of Toronto). The 3723 bp *Eco*RI fragment encoding the human eNOS cDNA was subcloned into the *Eco*RI site of pcDNA.3.1 to result in peNOS3.1. In frame integration was checked by RT-PCR and sequencing.

Plasmids were either linearized with *Apa*LI (pBra::eGFP) or *Rsr*II (pcDNA3.1, piNOS3.1 and peNOS3.1) and gel purified.

1 μg of each plasmid was stably transfected into the D3 ESC line with the Effectene transfection reagent from Qiagen during passaging as described (zur Nieden et al., 2005). The respective parental plasmids were used as mock controls. Clones were picked after antibiotic selection and plasmid integration was confirmed by PCR identification of the neomycin resistance cassette (5′-AGACAATCGGCTGCTCTGAT-3′; 5′-AGTGACAACGTCGAGCACAG-3′) generating T-Bra:GFP, $eNOS^+$, $iNOS^+$ and $[neo]^R$ ESC lines.

Luciferase reporter assay

Human embryonic kidney (HEK) 293T cells were routinely maintained in Dulbecco's Modified Eagle's Medium containing 10% fetal bovine serum, 50 U/ml penicillin and 50 mg/ml streptomycin (Invitrogen) in 5% CO_2 at 37℃. Cells were transiently transfected using calcium phosphate transfection and 500 ng of either the TOPflash or FOPflash reporter along with 500 ng of the GFP expression plasmid pvitro2 (Invitrogen). After 48 h, the transfection efficiency was monitored by GFP expression under a fluorescent microscope. Cells were then trypsinized, seeded into 24-well plates at a density of 1×10^5 cells/cm^2 and treated with NO modulators as indicated in the figure legends. Luciferase activity was measured after 24 h using a luciferase assay kit (Promega) according to the manufacturer's protocol.

Gene expression analysis

Gene expression analysis was performed using RT-PCR as previously described (zur Nieden et al., 2007b). Primer sequences were designed with primer 3 as specified below and were run through reverse ePCR (http://www.ncbi.nlm.nih.gov/sutils/e-pcr/reverse.cgi) to bioinformatically confirm amplicon identity. Annealing temperatures were 60℃, except for p53 (55℃). Primer sequences not noted in supplementary material Table S1 have been described previously (zur Nieden et al., 2003; zur Nieden et al., 2005; zur Nieden et al., 2007a). PCR products were semi-quantitatively analyzed using electrophoresis in 2 or 3% agarose gels containing 2% ethidium bromide. All gels were run in the presence of 1 bp plus ladder (Invitrogen) and a no-cDNA template control.

For quantitative PCR, the reaction composition and cycle conditions were modified as described (zur Nieden et al., 2007b). Dissociation curves were typically generated post-run for analysis of amplicon species.

Protein expression analysis

For the preparation of whole cell lysates, cells were harvested in radioimmunoprecipitation assay (RIPA) buffer (1% NP-40, 0.5% sodium deoxycholate, and 0.1% SDS in 1× PBS, pH 7.4) supplemented with protease inhibitor cocktail (1:100, Sigma) and phosphatase inhibitors sodium fluoride (10 mM, Sigma) and sodium vanadate (1 mM, Sigma). For preparation of nuclear and cytoplasmic fractions samples were purified using the ProteoJet Cytoplasmic and Nuclear Protein Extraction Kit (Fermentas) according to the manufacturer's instructions. Protein concentrations were assessed using the DC protein assay (Bio-Rad). Equal amounts of protein (50 μg) were then separated by SDS-PAGE and subsequently transferred to PVDF membranes. Membranes were blocked with 5% powdered milk in 1×Tris buffered saline (TBS) containing 0.1% Tween 20. Blots were probed with either a mouse monoclonal anti-CatnB antibody (1:1000, Invitrogen), a goat polyclonal anti-GFP antibody (1:500, Abcam), a mouse monoclonal anti-β-actin antibody (1:1000, Santa Cruz, Biotechnology), a mouse monoclonal anti-Tbp (1:2000, Abcam) or a mouse monoclonal anti-β-tubulin (1:500, Sigma) followed by horseradish peroxide-conjugated polyclonal anti-mouse (1:1000, Santa Cruz, Biotechnology) or anti-goat (1:1000, Invitrogen) IgG, and detected with the ECL Western Blotting detection kit (Amersham). Blots were then stripped in 100 mM 2-mercaptoethanol, 2% SDS, 62.5 mM Tris-HCl pH 6.7 at 50℃ for 1 h with occasional agitation and reprobed.

Flow cytometry

The percentage of GFP-expressing cells in T-Bra::GFP ESCs was measured by flow cytometry. Wild-type and T-Bra–GFP cells were differentiated in hanging drops, treated with NO modulating chemicals whereupon EBs were trypsinized into single cell suspensions on differentiation day 3.3. Wild-type cells were used to gate the appropriate population of interest and to gate out cellular autofluorescence. Ten thousand events were registered in a Beckman Coulter FC500 in FL1 and mean percentages of GFP-positive cells calculated from three independent differentiations.

Immunohistochemistry

Cells were washed with PBS and fixed with a 4% paraformaldehyde solution for 1 hour at 4℃. Subsequently, the cell membranes were permeabilized with 0.1% Triton X-100 in PBS for 15 min at room temperature. Non-specific binding of the antibodies was prevented by blocking in PBS containing 10% FBS and 0.1% BSA for 1 h at 37℃. Undifferentiated cells were identified through staining with a rabbit anti-Oct4 antibody (Abcam, 19857) and localization of CatnB was confirmed with an anti-CatnB antibody (Invitrogen, cat. no. 138400). Mature osteoblasts in ESC cultures were characterized with a mouse anti-osteocalcin (Chemicon, AB1857) and anti-osteoblast cadherin antibodies (Abcam, AB8999-1) over night at 4℃. Alexa-Fluor-488-conjugated anti-mouse (Invitrogen, A11001) or an Alexa-Fluor-546-conjugated anti-rabbit secondary antibodies (Invitrogen, A11071) were used to detect binding of the primary antibody. DNA was counterstained with 4′,6-diamidin-2′-phenylindoldihydrochlorid (Roche) at a concentration of 15 μM.

Tetracycline incorporation

Tetracycline was added to the culture medium at a final concentration of 35 μg/ml as described earlier (zur Nieden et al., 2003). Pictures were taken at a 10× magnification on Diagnostic Instrument's Olympus IX70 microscope with an

excitation in the UV channel to visualize yellow fluorescence indicative of incorporated tetracycline.

Biochemical analyses

Extracellular NO production was measured using a Griess-Diazo spectrophotometric assay. ESCs were preincubated in Phenol-Red-free medium for 24 h. Equal volumes of cell culture media and Griess reagent were incubated at room temperature for 15 minutes. Changes in absorbance were recorded at 540 nm. Triplicates of each biological sample were measured for each time-point and repeated twice daily from differentiation day 0 to 10. Intracellular NO was determined by incubation with 4 mM diaminofluorescein (DAF-2AD) at 37℃ for 30 minutes in Phenol-Red-free osteogenic medium containing NO agonists or antagonists. After photographing the cultures, cells were lysed in modified RIPA buffer (150 mM NaCl, 10 mM Tris, pH 7.2, 0.1% SDS, 1% Triton X-100, 1% deoxycholate, 5 mM EDTA) and subjected to fluorometric analysis at 495/535 nm.

Intracellular cGMP concentration was determined using an EIA kit from Cayman Chemicals (Michigan, USA). 100 EBs per treatment group were lysed with 0.1 M HCl and directly processed after acetylation. Absorbance of the yellow reaction products was measured at 405 nm and cGMP concentration was taken from a standard curve.

Alk Phos activity and Ca^{2+} content was measured from RIPA buffer lysates containing 1 mM phenylmethylsulfonyl fluoride, 10 mM benzamidine, 2 μg/ml leupeptin, 100 μM sodium orthovanadate and 10 mM p-nitrophenylphosphate as proteinase inhibitors. Lysates were collected from the plates after a 30 min incubation at 4℃ under gentle rocking. Samples were centrifuged and the RIPA supernatant collected for further analysis. The remaining cell pellet, which contained most of the mineral, was lysed with 1 N HCl overnight in the cold room.

RIPA and HCl lysates were then subjected to react with Arsenazo III reagent (DCL, Toronto, Canada) as described (zur Nieden et al., 2007a; Davis et al., 2011). A $CaCl_2$ standard was measured along with the samples at 650 nm in a Benchmark Plus microplate spectrophotometer (Bio-Rad). Absorbance readings for reagent only were subtracted in all instances. Amount of deposited calcium was expressed as a fraction of the total protein in the sample (Davis et al., 2011), which was measured from the RIPA lysates using DC protein assay reagent (Bio-Rad) with protocol as described therein. Samples were incubated with the reagent for 15 min and the change in absorbance was registered in a Benchmark Plus microplate spectrophotometer (Bio-Rad) at 750 nm. Protein quantities in samples were taken from a BSA standard curve.

Alkaline phosphatase activity was determined from the RIPA protein lysates only using p-nitrophenyl phosphate (Sigma) as described (zur Nieden et al., 2007b). The kinetic change in absorbance was measured at $t=0$ and $t=20$ min at 405 nm using a Bio-Rad Microplate Manager 5.2. Enzyme activity was calculated as described (Davis et al., 2011).

Bone explant culture

C57BL/6 mice were sacrificed according to an animal protocol of the University of California Riverside with CO_2 and subsequent cervical displacement. Femurs were collected and cleaned free of all tissue. PBS was flushed through the cavity of the bone to remove all bone marrow. Bone samples were then cut into small fragments with a surgical drill and then underwent several PBS washes to remove residual bone marrow cells. Bone slices were placed into 24-well plates and overlaid with ESC expansion and differentiation media.

$iNOS^+$ ESCs were labeled with the Qtracker 655 cell labeling kit (Molecular Probes/Invitrogen, Eugene, OR) in order to verify attachment to bone slices and ensure that the signal in all end point analysis could be attributed to the $iNOS^+$ ESCs differentiating into bone rather than the endogenous bone cells only. Briefly, trypsinized cells (1×10^6) were incubated with a 15 nM quantum dot (QD) labeling solution, made with ESC medium, for 60 min at 37℃ with periodic mixing. After incubation cells were washed three times with PBS, to remove any remaining QDs, and were immediately used in the co-culture experiment. Labeled cells (2.5×10^5) were slowly pipetted onto the bone slices. After 2 days, bone fragments were moved to new wells to minimize interference of unattached cells. Media were changed every other day.

Statistical analysis

Data are presented as means ± s.d. Comparison of two groups was made using Student's *t*-test for unpaired data. Comparison of more than two groups was conducted using ANOVA with $*P<0.1$, $**P<0.01$, $***P<0.001$ considered significant.

Acknowledgements

We thank the Canadian Institutes of Health Research Institute of Musculoskeletal Health and Arthritis/Pfizer for their early support of this project through a summer studentship awarded to R.M.G. We would further like to thank Dr Irving Weisman and Dr Scott Dylla (Stanford University) for the LEF/TCF reporter ESCs, Dr Philip A. Marsden (University of Toronto) for the eNOS plasmid and Dr Antje Kretschmar (Fraunhofer Institute for Cell Therapy and Immunology) for HEK293T cells. Finally, we are grateful to Dr Guoliang Meng, Sylvia Taube, Beatrice Kuske, Anne Findeisen and Virginia Donovan for technical assistance.

Funding

This work was supported by a postdoctoral fellowship [grant number 200200727 to N.z.N.] and a Senior Scholarship [grant number 20040232 to D.E.R.] from the Alberta Heritage Foundation for Medical Research; and the German Federal Ministry for Science and Research (BMBF) [grant number 0313453 to N.z.N.].

Supplementary material available online at
http://jcs.biologists.org/lookup/suppl/doi:10.1242/jcs.081703/-/DC1

References

Achan, V., Tran, C. T. L., Arrigoni, F., Whitley, G. S., Leiper, J. M. and Vallance, P. (2002). All-trans-retinoic acid increases nitric oxide synthesis by endothelial cells: a role for the induction of dimethylarginine dimethylaminohydrolase. *Circ. Res.* **90**, 764-769.

Adewumi, O., Aflatoonian, B., Ahrlund-Richter, L., Amit, M., Andrews, P. W., Beighton, G., Bello, P. A., Benvenisty, N., Berry, L. S., Bevan, S. et al. (2007). Characterization of human embryonic stem cell lines by the International Stem Cell Initiative. *Nat. Biotechnol.* **25**, 803-816.

Aguirre, J., Buttery, L., O'Shaughnessy, M., Afzal, F., Fernandez de Marticorena, I., Hukkanen, M., Huang, P., MacIntyre, I. and Polak, J. (2001). Endothelial nitric oxide synthase gene-deficient mice demonstrate marked retardation in postnatal bone formation, reduced bone volume, and defects in osteoblast maturation and activity. *Am. J. Pathol.* **158**, 247-257.

Armour, K. J., Armour, K. E., van't Hof, R. J., Reid, D. M., Wei, X. Q., Liew, F. Y. and Ralston, S. H. (2001). Activation of the inducible nitric oxide synthase pathway contributes to inflammation-induced osteoporosis by suppressing bone formation and causing osteoblast apoptosis. *Arthritis Rheum.* **44**, 2790-2796.

Arnold, S. J., Stappert, J., Bauer, A., Kispert, A., Herrmann, B. G. and Kemler, R. (2000). Brachyury is a target gene of the Wnt/beta-catenin signaling pathway. *Mech. Dev.* **91**, 249-258.

Bielby, R. C., Boccaccini, A. R., Polak, J. M. and Buttery, L. D. (2004). In vitro differentiation and in vivo mineralization of osteogenic cells derived from human embryonic stem cells. *Tissue Eng.* **10**, 1518-1525.

Blum, M., Gaunt, S. J., Cho, K. W. Y., Steinbeisser, H., Blumberg, B., Bittner, D. and De Robertis, E. M. (1992). Gastrulation in the mouse: the role of the homeobox gene goosecoid. *Cell* **69**, 1097-1106.

Buttery, L. D., Bourne, S., Xynos, J. D., Wood, H., Hughes, F. J., Hughes, S. P., Episkopou, V. and Polak, J. M. (2001). Differentiation of osteoblasts and in vitro bone formation from murine embryonic stem cells. *Tissue Eng.* **7**, 89-99.

Casero, E., Martín-Gago, J. A., Pariente, F. and Lorenzo, E. (2004). Metal release in metallothioneins induced by nitric oxide: X-ray absorption spectroscopy study. *Eur. Biophys. J.* **33**, 726-731.

Chae, H. J., Park, R. K., Chung, H. T., Kang, J. S., Kim, M. S., Choi, D. Y., Bang, B. G. and Kim, H. R. (1997). Nitric oxide is a regulator of bone remodelling. *J. Pharm. Pharmacol.* **49**, 897-902.

Chapman, D. L. and Papaioannou, V. E. (1998). Three neural tubes in mouse embryos with mutations in the T-box gene Tbx6. *Nature* **391**, 695-697.

Chen, U., Kosco, M. and Staerz, U. (1992). Establishment and characterization of lymphoid and myeloid mixed-cell populations from mouse late embryoid bodies, "embryonic-stem-cell fetuses". *Proc. Natl. Acad. Sci. USA* **89**, 2541-2545.

Cheng, Z., Tseng, Y. and White, M. F. (2010). Insulin signaling meets mitochondria in metabolism. *Trends Endocrinol. Metab.* **21**, 589-598.

Chiche, J. D., Schlutsmeyer, S. M., Bloch, D. B., de la Monte, S. M., Roberts, J. D., Jr, Filippov, G., Janssens, S. P., Rosenzweig, A. and Bloch, K. D. (1998). Adenovirus-mediated gene transfer of cGMP-dependent protein kinase increases the sensitivity of cultured vascular smooth muscle cells to the antiproliferative and pro-apoptotic effects of nitric oxide/cGMP. *J. Biol. Chem.* **273**, 34263-34271.

Cui, X., Zhang, J., Ma, P., Myers, D. E., Goldberg, I. G., Sittler, K. J., Barb, J. J., Munson, P. J., Cintron, A. P., McCoy, J. P. et al. (2005). cGMP-independent nitric oxide signaling and regulation of the cell cycle. *BMC Genomics* **6**, 151.

Damalas, A., Ben-Ze'ev, A., Simcha, I., Shtutman, M., Leal, J. F., Zhurinsky, J., Geiger, B. and Oren, M. (1999). Excess beta-catenin promotes accumulation of transcriptionally active p53. *EMBO J.* **18**, 3054-3063.

Davis, L. A. and zur Nieden, N. I. (2008). Mesodermal fate decisions of a stem cell: the Wnt switch. *Cell. Mol. Life Sci.* **65**, 2658-2674.

Davis, L. A., Dienelt, A. and zur Nieden, N. I. (2011). Absorption-based assays for the analysis of osteogenic and chondrogenic yield. *Methods Mol. Biol.* **690**, 255-272.

Dhakshinamoorthy, S., Sridharan, S. R., Li, L., Ng, P. Y., Boxer, L. M. and Porter, A. G. (2007). Protein/DNA arrays identify nitric oxide-regulated cis-element and trans-factor activities some of which govern neuroblastoma cell viability. *Nucleic Acids Res.* **35**, 5439-5451.

Dodd-o, J. M., Zheng, G., Silverman, H. S., Lakatta, E. G. and Ziegelstein, R. C. (1997). Endothelium-independent relaxation of aortic rings by the nitric oxide synthase inhibitor diphenyleneiodonium. *Br. J. Pharmacol.* **120**, 857-864.

Du, Q., Park, K. S., Guo, Z., He, P., Nagashima, M., Shao, L., Sahai, R., Geller, D. A. and Hussain, S. P. (2006). Regulation of human nitric oxide synthase 2 expression by Wnt beta-catenin signaling. *Cancer Res.* **66**, 7024-7031.

Dush, M. K. and Martin, G. R. (1992). Analysis of mouse Evx genes: Evx-1 displays graded expression in the primitive streak. *Dev. Biol.* **151**, 273-287.

Evans, D. M. and Ralston, S. H. (1996). Nitric oxide and bone. *J. Bone Miner. Res.* **11**, 300-305.

Fehling, H. J., Lacaud, G., Kubo, A., Kennedy, M., Robertson, S., Keller, G. and Kouskoff, V. (2003). Tracking mesoderm induction and its specification to the hemangioblast during embryonic stem cell differentiation. *Development* **130**, 4217-4227.

Forlani, S., Lawson, K. A. and Deschamps, J. (2003). Acquisition of Hox codes during gastrulation and axial elongation in the mouse embryo. *Development* **130**, 3807-3819.

Forrester, K., Ambs, S., Lupold, S. E., Kapust, R. B., Spillare, E. A., Weinberg, W. C., Felley-Bosco, E., Wang, X. W., Geller, D. A., Tzeng, E. et al. (1996). Nitric oxide-induced p53 accumulation and regulation of inducible nitric oxide synthase expression by wild-type p53. *Proc. Natl. Acad. Sci. USA* **93**, 2442-2447.

Förstermann, U. and Neufang, B. (1984). The endothelium-dependent vasodilator effect of acetylcholine: characterization of the endothelial relaxing factor with inhibitors of arachidonic acid metabolism. *Eur. J. Pharmacol.* **10**, 65-70.

Fukumoto, S., Hsieh, C. M., Maemura, K., Layne, M. D., Yet, S. F., Lee, K. H., Matsui, T., Rosenzweig, A., Taylor, W. G., Rubin, J. S. et al. (2001). Akt participation in the Wnt signaling pathway through Dishevelled. *J. Biol. Chem.* **276**, 17479-17483.

Gadue, P., Huber, T. L., Paddison, P. J. and Keller, G. M. (2006). Wnt and TGF-beta signaling are required for the induction of an in vitro model of primitive streak formation using embryonic stem cells. *Proc. Natl. Acad. Sci. USA* **103**, 16806-16811.

Hallonet, M., Kaestner, K. H., Martin-Parras, L., Sasaki, H., Betz, U. A. and Ang, S. L. (2002). Maintenance of the specification of the anterior definitive endoderm and forebrain depends on the axial mesendoderm: a study using HNF3beta/Foxa2 conditional mutants. *Dev. Biol.* **243**, 20-33.

Huelsken, J., Vogel, R., Brinkmann, V., Erdmann, B., Birchmeier, C. and Birchmeier, W. (2000). Requirement for β-catenin in anterior-posterior axis formation in mice. *J. Cell Biol.* **148**, 567-578.

Hukkanen, M., Hughes, F. J., Buttery, L. D., Gross, S. S., Evans, T. J., Seddon, S., Riveros-Moreno, V., Macintyre, I. and Polak, J. M. (1995). Cytokine-stimulated expression of inducible nitric oxide synthase by mouse, rat, and human osteoblast-like cells and its functional role in osteoblast metabolic activity. *Endocrinology* **136**, 5445-5453.

Ignarro, L. J., Lippton, H., Edwards, J. C., Baricos, W. H., Hyman, A. L., Kadowitz, P. J. and Gruetter, C. A. (1981). Mechanism of vascular smooth muscle relaxation by organic nitrates, nitrites, nitroprusside and nitric oxide: evidence for the involvement of S-nitrosothiols as active intermediates. *J. Pharmacol. Exp. Ther.* **218**, 739-749.

Jiang, X., Gwye, Y., McKeown, S. J., Bronner-Fraser, M., Lutzko, C. and Lawlor, E. R. (2009). Isolation and characterization of neural crest stem cells derived from in vitro-differentiated human embryonic stem cells. *Stem Cells Dev.* **18**, 1059-1070.

Keller, K. C. and zur Nieden, N. I. (2011). Osteogenesis from pluripotent stem cells: neural crest or mesodermal origin? In *Embryonic Stem Cells - Differentiation and Pluripotent Alternatives* (ed. M. S. Kallos), pp 323-348. Rijeka, HR: InTech Publishers.

Kuboki, K., Jiang, Z. Y., Takahara, N., Ha, S. W., Igarashi, M., Yamauchi, T., Feener, E. P., Herbert, T. P., Rhodes, C. J. and King, G. L. (2000). Regulation of endothelial constitutive nitric oxide synthase gene expression in endothelial cells and in vivo: a specific vascular action of insulin. *Circulation* **101**, 676-681.

Leiper, J. M., Santa Maria, J., Chubb, A., MacAllister, R. J., Charles, I. G., Whitley, G. S. and Vallance, P. (1999). Identification of two human dimethylarginine dimethylaminohydrolases with distinct tissue distributions and homology with microbial arginine deiminases. *Biochem. J.* **343**, 209-214.

Li, Q., Dashwood, W. M., Zhong, X., Al-Fageeh, M. and Dashwood, R. H. (2004). Cloning of the rat beta-catenin gene (Ctnnb1) promoter and its functional analysis compared with the Catnb and CTNNB1 promoters. *Genomics* **83**, 231-242.

Lin, S. K., Kok, S. H., Kuo, M. Y., Lee, M. S., Wang, C. C., Lan, W. H., Hsiao, M., Goldring, S. R. and Hong, C. Y. (2003). Nitric oxide promotes infectious bone resorption by enhancing cytokine-stimulated interstitial collagenase synthesis in osteoblasts. *J. Bone Miner. Res.* **18**, 39-46.

Lincoln, T. M. and Cornwell, T. L. (1993). Intracellular cyclic GMP receptor proteins. *FASEB J.* **7**, 328-338.

Liu, P., Wakamiya, M., Shea, M. J., Albrecht, U., Behringer, R. R. and Bradley, A. (1999). Requirement for Wnt3 in vertebrate axis formation. *Nat. Genet.* **22**, 361-365.

Loweth, A. C., Williams, G. T., Scarpello, J. H. and Morgan, N. G. (1997). Evidence for the involvement of cGMP and protein kinase G in nitric oxide-induced apoptosis in the pancreatic B-cell line, HIT-T15. *FEBS Lett.* **400**, 285-288.

Lyashenko, N., Winter, M., Migliorini, D., Biechele, T., Moon, R. T. and Hartmann, C. (2011). Differential requirement for the dual functions of β-catenin in embryonic stem cell self-renewal and germ layer formation. *Nat. Cell Biol.* **13**, 753-761.

McCall, T. B., Feelisch, M., Palmer, R. M. and Moncada, S. (1991). Identification of N-iminoethyl-L-ornithine as an irreversible inhibitor of nitric oxide synthase in phagocytic cells. *Br. J. Pharmacol.* **102**, 234-238.

Mendes, A. F., Carvalho, A. P., Caramona, M. M. and Lopes, M. C. (2001). Diphenyleneiodonium inhibits NF-kappaB activation and iNOS expression induced by IL-1beta: involvement of reactive oxygen species. *Mediators Inflamm.* **10**, 209-215.

Moon, R. T., Bowerman, B., Boutros, M. and Perrimon, N. (2002). The promise and perils of Wnt signaling through beta-catenin. *Science* **296**, 1644-1646.

Mora-Castilla, S., Tejedo, J. R., Hmadcha, A., Cahuana, G. M., Martín, F., Soria, B. and Bedoya, F. J. (2010). Nitric oxide repression of Nanog promotes mouse embryonic stem cell differentiation. *Cell Death Differ.* **17**, 1025-1033.

Mujoo, K., Sharin, V. G., Bryan, N. S., Krumenacker, J. S., Sloan, C., Parveen, S., Nikonoff, L. E., Kots, A. Y. and Murad, F. (2008). Role of nitric oxide signaling components in differentiation of embryonic stem cells into myocardial cells. *Proc. Natl. Acad. Sci. USA* **105**, 18924-18929.

Nakanishi, M., Kurisaki, A., Hayashi, Y., Warashina, M., Ishiura, S., Kusuda-Furue, M. and Asashima, M. (2009). Directed induction of anterior and posterior primitive streak by Wnt from embryonic stem cells cultured in a chemically defined serum-free medium. *FASEB J.* **23**, 114-122.

Nath, N., Labaze, G., Rigas, B. and Kashfi, K. (2005). NO-donating aspirin inhibits the growth of leukemic Jurkat cells and modulates beta-catenin expression. *Biochem. Biophys. Res. Commun.* **326**, 93-99.

Ogawa, T., Kimoto, M., Watanabe, H. and Sasaoka, K. (1987). Metabolism of NG,NG- and NG,N'G-dimethylarginine in rats. *Arch. Biochem. Biophys.* **252**, 526-537.

Ogawa, T., Kimoto, M. and Sasaoka, K. (1989). Purification and properties of a new enzyme, NG,NG-dimethylarginine dimethylaminohydrolase, from rat kidney. *J. Biol. Chem.* **264**, 10205-10209.

Orr-Urtreger, A., Bedford, M. T., Do, M. S., Eisenbach, L. and Lonai, P. (1992). Developmental expression of the alpha receptor for platelet-derived growth factor, which is deleted in the embryonic lethal Patch mutation. *Development* **115**, 289-303.

Padmasekar, M., Sharifpanah, F., Finkensieper, A., Wartenberg, M. and Sauer, H. (2011). Stimulation of cardiomyogenesis of embryonic stem cells by nitric oxide downstream of AMP-activated protein kinase and mTOR signaling pathways. *Stem Cells Dev.* **20**, 2163-2175.

Papapetropoulos, A., Rudic, R. D. and Sessa, W. C. (1999). Molecular control of nitric oxide synthases in the cardiovascular system. *Cardiovasc. Res.* **43**, 509-520.

Pearce, L. L., Gandley, R. E., Han, W., Wasserloos, K., Stitt, M., Kanai, A. J., McLaughlin, M. K., Pitt, B. R. and Levitan, E. S. (2000). Role of metallothionein in nitric oxide signaling as revealed by a green fluorescent fusion protein. *Proc. Natl. Acad. Sci. USA* **97**, 477-482.

Phillips, B. W., Belmonte, N., Vernochet, C., Ailhaud, G. and Dani, C. (2001). Compactin enhances osteogenesis in murine embryonic stem cells. *Biochem. Biophys. Res. Commun.* **284**, 478-484.

Rees, D. D., Palmer, R. M., Schulz, R., Hodson, H. F. and Moncada, S. (1990). Characterization of three inhibitors of endothelial nitric oxide synthase in vitro and in vivo. *Br. J. Pharmacol.* **101**, 746-752.

Sadot, E., Geiger, B., Oren, M. and Ben-Ze'ev, A. (2001). Down-regulation of β-catenin by activated p53. *Mol. Cell. Biol.* **21**, 6768-6781.

Salmanian, S., Najafi, S. M., Rafipour, M., Arjomand, M. R., Shahheydari, H., Ansari, S., Kashkooli, L., Rasouli, S. J., Jazi, M. S. and Minaei, T. (2010). Regulation of GSK-3beta and beta-Catenin by Galphaq in HEK293T cells. *Biochem. Biophys. Res. Commun.* **395**, 577-582.

Sellak, H., Yang, X., Cao, X., Cornwell, T., Soff, G. A. and Lincoln, T. (2002). Sp1 transcription factor as a molecular target for nitric oxide— and cyclic nucleotide—mediated suppression of cGMP-dependent protein kinase-Ialpha expression in vascular smooth muscle cells. *Circ. Res.* **90**, 405-412.

Seo, J. H., Sung, H. J., Choi, C. W., Kim, B. S., Shin, S. W., Kim, Y. H., Min, B. H. and Kim, J. S. (2008). Extrinsic nitric oxide donor partially reverses arginine deiminase induced cell growth inhibition through NFkappaB and Bcl-X L. *Invest. New Drugs* **26**, 277-282.

Shimojo, T., Hiroe, M., Ishiyama, S., Ito, H., Nishikawa, T. and Marumo, F. (1999). Nitric oxide induces apoptotic death of cardiomyocytes via a cyclic-GMP-dependent pathway. *Exp. Cell Res.* **247**, 38-47.

Shtutman, M., Zhurinsky, J., Simcha, I., Albanese, C., D'Amico, M., Pestell, R. and Ben-Ze'ev, A. (1999). The cyclin D1 gene is a target of the beta-catenin/LEF-1 pathway. *Proc. Natl. Acad. Sci. USA* **96**, 5522-5527.

Smolenski, A., Burkhardt, A. M., Eigenthaler, M., Butt, E., Gambaryan, S., Lohmann, S. M. and Walter, U. (1998). Functional analysis of cGMP-dependent protein kinases I and II as mediators of NO/cGMP effects. *Naunyn Schmiedebergs Arch. Pharmacol.* **358**, 134-139.

Sottile, V., Thomson, A. and McWhir, J. (2003). In vitro osteogenic differentiation of human ES cells. *Cloning Stem Cells* **5**, 149-155.

Spallotta, F., Rosati, J., Straino, S., Nanni, S., Grasselli, A., Ambrosino, V., Rotili, D., Valente, S., Farsetti, A., Mai, A. et al. (2010). Nitric oxide determines mesodermic differentiation of mouse embryonic stem cells by activating class IIa histone deacetylases: potential therapeutic implications in a mouse model of hindlimb ischemia. *Stem Cells* **28**, 431-442.

St Croix, C. M., Wasserloos, K. J., Dineley, K. E., Reynolds, I. J., Levitan, E. S. and Pitt, B. R. (2002). Nitric oxide-induced changes in intracellular zinc homeostasis are mediated by metallothionein/thionein. *Am. J. Physiol. Lung Cell Mol. Physiol.* **282**, L185-L192.

Stacey, P., Rulten, S., Dapling, A. and Phillips, S. C. (1998). Molecular cloning and expression of human cGMP-binding cGMP-specific phosphodiesterase (PDE5). *Biochem. Biophys. Res. Commun.* **247**, 249-254.

Stuehr, D. J., Fasehun, O. A., Kwon, N. S., Gross, S. S., Gonzalez, J. A., Levi, R. and Nathan, C. F. (1991). Inhibition of macrophage and endothelial cell nitric oxide synthase by diphenyleneiodonium and its analogs. *FASEB J.* **5**, 98-103.

Su, F., Overholtzer, M., Besser, D. and Levine, A. J. (2002). WISP-1 attenuates p53-mediated apoptosis in response to DNA damage through activation of the Akt kinase. *Genes Dev.* **16**, 46-57.

Takakura, N., Yoshida, H., Ogura, Y., Kataoka, H., Nishikawa, S. and Nishikawa, S. (1997). PDGFR alpha expression during mouse embryogenesis: immunolocalization analyzed by whole-mount immunohistostaining using the monoclonal anti-mouse PDGFR alpha antibody APA5. *J. Histochem. Cytochem.* **45**, 883-893.

Trettner, S., Seeliger, A. and zur Nieden, N. I. (2011). Embryoid body formation: recent advances in automated bioreactor technology. *Methods Mol. Biol.* **690**, 135-149.

van Noort, M., Meeldijk, J., van der Zee, R., Destree, O. and Clevers, H. (2002). Wnt signaling controls the phosphorylation status of beta-catenin. *J. Biol. Chem.* **277**, 17901-17905.

Wang, Y. X., Poon, C. I., Poon, K. S. and Pang, C. C. (1993). Inhibitory actions of diphenyleneiodonium on endothelium-dependent vasodilatations in vitro and in vivo. *Br. J. Pharmacol.* **110**, 1232-1238.

Wang, H., Wang, Z., Chen, J. and Wu, J. (2007). Apoptosis induced by NO via phosphorylation of p38 MAPK that stimulates NF-kappaB, p53 and caspase-3 activation in rabbit articular chondrocytes. *Cell Biol. Int.* **31**, 1027-1035.

Wang, H., Zhang, R., Wen, S., McCafferty, D. M., Beck, P. L. and MacNaughton, W. K. (2009). Nitric oxide increases Wnt-induced secreted protein-1 (WISP-1/CCN4) expression and function in colitis. *J. Mol. Med.* **87**, 435-445.

Williams, J. L., Nath, N., Chen, J., Hundley, T. R., Gao, J., Kopelovich, L., Kashfi, K. and Rigas, B. (2003). Growth inhibition of human colon cancer cells by nitric oxide (NO)-donating aspirin is associated with cyclooxygenase-2 induction and beta-catenin/T-cell factor signaling, nuclear factor-kappaB, and NO synthase 2 inhibition: implications for chemoprevention. *Cancer Res.* **63**, 7613-7618.

Wittler, L., Shin, E. H., Grote, P., Kispert, A., Beckers, A., Gossler, A., Werber, M. and Herrmann, B. G. (2007). Expression of Msgn1 in the presomitic mesoderm is controlled by synergism of WNT signalling and Tbx6. *EMBO Rep.* **8**, 784-789.

Wobus, A. M., Wallukat, G. and Hescheler, J. (1991). Pluripotent mouse embryonic stem cells are able to differentiate into cardiomyocytes expressing chronotropic responses to adrenergic and cholinergic agents and Ca2+ channel blockers. *Differentiation* **48**, 173-182.

Yamaguchi, T. P., Takada, S., Yoshikawa, Y., Wu, N. and McMahon, A. P. (1999). T (Brachyury) is a direct target of Wnt3a during paraxial mesoderm specification. *Genes Dev.* **13**, 3185-3190.

Zecchin, H. G., Priviero, F. B., Souza, C. T., Zecchin, K. G., Prada, P. O., Carvalheira, J. B., Velloso, L. A., Antunes, E. and Saad, M. J. (2007). Defective insulin and acetylcholine induction of endothelial cell-nitric oxide synthase through insulin receptor substrate/Akt signaling pathway in aorta of obese rats. *Diabetes* **56**, 1014-1024.

Zeng, G. and Quon, M. J. (1996). Insulin-stimulated production of nitric oxide is inhibited by wortmannin. Direct measurement in vascular endothelial cells. *J. Clin. Invest.* **98**, 894-898.

zur Nieden, N. I., Kempka, G. and Ahr, H. J. (2003). In vitro differentiation of embryonic stem cells into mineralized osteoblasts. *Differentiation* **71**, 18-27.

zur Nieden, N. I., Kempka, G., Rancourt, D. E. and Ahr, H. J. (2005). Induction of chondro-, osteo- and adipogenesis in embryonic stem cells by bone morphogenetic protein-2: effect of cofactors on differentiating lineages. *BMC Dev. Biol.* **5**, 1.

zur Nieden, N. I., Price, F. D., Davis, L. A., Everitt, R. E. and Rancourt, D. E. (2007a). Gene profiling on mixed embryonic stem cell populations reveals a biphasic role for beta-catenin in osteogenic differentiation. *Mol. Endocrinol.* **21**, 674-685.

zur Nieden, N. I., Cormier, J. T., Rancourt, D. E. and Kallos, M. S. (2007b). Embryonic stem cells remain highly pluripotent following long term expansion as aggregates in suspension bioreactors. *J. Biotechnol.* **129**, 421-432.